Regulation of Light Harvesting in Chlamydomonas reinhardtii Two Protein Phosphatases Are Involved in State Transitions

Federica Cariti, Marie Chazaux, Linnka Lefebvre-Legendre, Paolo Longoni, Bart Ghysels, Xenie Johnson, Michel Goldschmidt-Clermont

Regulation of Light Harvesting in *Chlamydomonas reinhardtii* Two Protein Phosphatases Are Involved in State Transitions[1][OPEN]

Federica Cariti,[a] Marie Chazaux,[b] Linnka Lefebvre-Legendre,[a] Paolo Longoni,[c,2] Bart Ghysels,[b,3] Xenie Johnson,[b] and Michel Goldschmidt-Clermont[c,4,5]

[a]Department of Botany and Plant Biology, University of Geneva, 1211, Geneva 4, Switzerland
[b]Aix Marseille University, Commissariat à l'Énergie Atomique et aux Énergies Alternatives, Centre National de la Recherche Scientifique, Biosciences and Biotechnologies Institute of Aix-Marseille, F–13108 Saint Paul-Lez-Durance, France
[c]Institute of Genetics and Genomics of Geneva, University of Geneva, 1205 Geneva 4, Switzerland

ORCID IDs: 0000-0002-1970-9832 (F.C.); 0000-0002-5023-2948 (M.C.); 0000-0003-0587-7621 (P.L.); 0000-0003-3424-7047 (X.J.); 0000-0003-1224-5868 (M.G.-C.).

Protein phosphorylation plays important roles in short-term regulation of photosynthetic electron transfer, and during state transitions, the kinase STATE TRANSITION7 (STT7) of *Chlamydomonas reinhardtii* phosphorylates components of light-harvesting antenna complex II (LHCII). This reversible phosphorylation governs the dynamic allocation of a part of LHCII to PSI or PSII, depending on light conditions and metabolic demands, but counteracting phosphatase(s) remain unknown in *C. reinhardtii*. Here we analyzed state transitions in *C. reinhardtii* mutants of two phosphatases, PROTEIN PHOSPHATASE1 and PHOTOSYSTEM II PHOSPHATASE, which are homologous to proteins that antagonize the state transition kinases (STN7 and STN8) in Arabidopsis (*Arabidopsis thaliana*). The transition from state 2 to state 1 was retarded in *pph1*, and surprisingly also in *pbcp*. However, both mutants eventually returned to state 1. In contrast, the double mutant *pph1;pbcp* appeared strongly locked in state 2. The complex phosphorylation patterns of the LHCII trimers and of the monomeric subunits were affected in the phosphatase mutants. Their analysis indicated that the two phosphatases have different yet overlapping sets of protein targets. The dual control of thylakoid protein dephosphorylation and the more complex antenna phosphorylation patterns in *C. reinhardtii* compared to Arabidopsis are discussed in the context of the stronger amplitude of state transitions and the more diverse LHCII isoforms in the alga.

[1]This work was supported by the European Commission's Marie Curie Initial Training Network project (AcclimPhot grant no. PITN–GA–2012–316427); the University of Geneva; the Institute of Genetics and Genomics of Geneva; the Swiss National Science Foundation (grant no. SNF–31003A–146300); the European Commission's European FP6 program (SOLAR-H grant no. STRP516510); the Agence Nationale pour la Recherche (ChloroPaths grant no. ANR–14–CE05–0041–01); and the French Ministry of Science and Education.

[2]Present address: Université de Neuchâtel, 2000 Neuchâtel, Switzerland.

[3]Present address: Université de Liège, Laboratoire de Bioénergétique, 4000 Liège, Belgium.

[4]Author for contact: michel.goldschmidt-clermont@unige.ch.

[5]Senior author.

The author responsible for distribution of materials integral to the findings presented in this article in accordance with the policy described in the Instructions for Authors (www.plantphysiol.org) is: Michel Goldschmidt-Clermont (michel.goldschmidt-clermont@unige.ch).

M.G.-C. and X.J. conceived and coordinated the research project; F.C., M.C., L.L.-L., M.G.-C., P.L., and B.G. performed the experiments and analyzed the data; M.G.-C. and F.C. wrote the article with contributions of all the authors.

[OPEN]Articles can be viewed without a subscription.

www.plantphysiol.org/cgi/doi/10.1104/pp.20.00384

To fulfill their energy requirements, photoautotrophic plants and algae rely on a photosynthetic electron transfer chain embedded in the thylakoid membrane of the chloroplast. Two photosystems (PSII and PSI) and their associated light-harvesting antennae complexes (LHCII and LHCI) mediate the conversion of light energy into chemical energy. In the linear mode of electron flow, PSII and PSI work in series to extract electrons from water and to reduce ferredoxin (Fd) and NADPH. The two photosystems are connected through the plastoquinone (PQ) pool, the cytochrome b_6f complex, and plastocyanin. Electron transfer along the chain is coupled to proton accumulation in the luminal compartment of the thylakoid membranes, and the resulting proton gradient is used to drive ATP synthesis. In the cyclic mode of electron flow (CEF), which involves PSI and the cytochrome b_6f complex, ATP is produced but there is no net reduction of Fd and $NADP^+$. The chemical energy that is stored in ATP, the condition of reduced Fd, and the presence of NADPH fuels cell metabolism, and in particular the synthesis of storage compounds such as carbohydrates. In the dark or in sink tissues, these compounds can, in

turn, provide energy through glycolysis, respiration, or fermentation.

While the photosystems are highly conserved in evolution, the light-harvesting antennae and their organization within the photosynthetic supercomplexes are more diverse. In plants, LHCI is constituted of four monomeric subunits (Lhca1–Lhca4) stably associated with PSI, while in *Chlamydomonas reinhardtii*, LHCI is composed of 10 subunits, consisting of two LHCA1 and one each of LHCA2–LHCA9 (Takahashi et al., 2004; Drop et al., 2011; Mazor et al., 2015; Ozawa et al., 2018; Kubota-Kawai et al., 2019). LHCII in plants is composed of trimers containing combinations of Lhcb1, Lhcb2, and Lhcb3, and of monomeric subunits Lhcb4 (CP29), Lhcb5 (CP26), and Lhcb6 (CP24). In *C. reinhardtii*, the LHCII trimers are made of eight different subunits encoded by nine genes, LHCBM1 to LHCBM9, with LHCBM2 and LHCBM7 sharing an identical amino acid sequence, while there are only two types of monomeric subunits, LHCB4 and LHCB5 (Elrad and Grossman, 2004; Merchant et al., 2007; reviewed by Minagawa and Takahashi, 2004; Crepin and Caffarri, 2018).

Both external and internal factors induce responses that regulate the activity of the photosynthetic machinery (Eberhard et al., 2008). External conditions of temperature and light vary widely, over timescales that range from months for changes linked to the seasons, to minutes or seconds for those related to the weather or the patchy shade of a canopy. Rapid variations in light are challenging for photosynthetic organisms, which have to optimize light harvesting when photon flux is limiting but avoid photodamage when light is in excess. The internal demand for ATP or reducing power can also vary widely and rapidly depending on metabolic activities, so that electron transport has to be adapted accordingly through regulatory responses of the photosynthetic machinery (Yamori and Shikanai, 2016).

Under limiting light, the mechanism of state transitions is an important regulator for the redox balance of the electron transport chain, through the reversible allocation of a part of LHCII to either PSII or PSI (Rochaix, 2014). In state 1 (St 1), this mobile part of the antenna is connected to PSII, while in St 2 it is at least in part connected to PSI (Nagy et al., 2014; Ünlü et al., 2014; Wlodarczyk et al., 2015; Nawrocki et al., 2016; Iwai et al., 2018). State transitions represent a negative feedback regulatory loop that is important for maintaining the redox homeostasis of the PQ pool: Reduction of the pool favors St 2 leading to an increase in the cross section of the antenna connected to PSI, whose activity oxidizes the pool. Conversely, oxidation of the PQ pool favors St 1 leading to an increase in the cross section of PSII, which promotes reduction of the pool. Under normal conditions, the system maintains an intermediate state between St 1 and St 2, which ensures a balanced ratio of reduced and oxidized PQ (Goldschmidt-Clermont and Bassi, 2015). In land plants such as Arabidopsis (*Arabidopsis thaliana*), state transitions operate under low light in response to changes in light quality, for example under a canopy where the spectrum is enriched in far-red light, which is more efficiently absorbed by PSI than PSII. Thus, St 1 can be experimentally favored by illumination with far-red light, while St 2 is promoted by blue light. In *C. reinhardtii*, the difference in spectral properties of the two photosystems is not as pronounced (Tapie et al., 1984). However, a strong transition toward St 2 involving a large part of the LHCII antenna is promoted by anaerobiosis in the dark (Wollman and Delepelaire, 1984; Bulte and Wollman, 1990). For lack of oxygen, production of ATP by mitochondrial respiration is prevented, as well as PQH_2 oxidation by chloroplast PLASTID TERMINAL OXIDASE, while fermentative metabolism produces an excess of reducing equivalents leading to a strong reduction of the PQ pool (Bulte et al., 1990; Houille-Vernes et al., 2011). CEF is tuned by redox conditions independently of state transitions (Takahashi et al., 2013). However, by favoring the activity of PSI, St 2 will enhance CEF and the production of ATP, at the expense of the linear mode of electron flow and the production of reducing power, which depend on PSII (Finazzi et al., 2002).

The transition toward St 2 is regulated through phosphorylation of LHCII by the protein kinase STATE TRANSITION7 (STN7) in land plants (Bellafiore et al., 2005), or its ortholog STT7 in *C. reinhardtii* (Fleischmann et al., 1999; Depège et al., 2003; Lemeille et al., 2010). The activation of this kinase requires an interaction with the stromal side of the cytochrome b_6f complex and the docking of PQH_2 to the Q_o site of the complex (Vener et al., 1997; Zito et al., 1999; Dumas et al., 2017). The process is rapidly reversible, because the kinase is counteracted by the protein phosphatase PROTEIN PHOSPHATASE1/THYLAKOID ASSOCIATED PHOSPHATASE38 (PPH1/TAP38) in land plants (Pribil et al., 2010; Shapiguzov et al., 2010), which favors the transition toward St 1. In Arabidopsis, the PSI–LHCI–LHCII supercomplex, which is characteristic of St 2, contains one LHCII trimer that belongs to a pool that would be loosely associated with PSII in St 1 (L trimers; Galka et al., 2012). This trimer contains both Lhcb1 and Lhcb2 subunits, but it is the phosphorylation of the Lhcb2 isoform that is crucial for state transitions by favoring docking of the LHCII trimer to PSI (Pietrzykowska et al., 2014; Crepin and Caffarri, 2015; Longoni et al., 2015; Pan et al., 2018). Recently, PSI–LHCI–LHCII complexes with a second LHCII trimer have been observed (Benson et al., 2015; Yadav et al., 2017). In *C. reinhardtii*, STT7 phosphorylates several subunits of LHCII trimers, and also the monomeric antenna LHCB4 (CP29; Turkina et al., 2006; Lemeille et al., 2010). The other monomeric antenna, LHCB5 (CP26) can also be phosphorylated in this alga (Bassi and Wollman, 1991). In *C. reinhardtii*, the PSI–LHCI–LHCII complex involves one or two LHCII trimers, and strikingly also the monomeric antennae LHCB4 (CP29) and LHCB5 (CP26; Takahashi et al., 2006). The LHCBM5 isoform of LHCII is particularly enriched in this complex, but other LHCBM subunits appear to also

participate in its formation and to be phosphorylated (Drop et al., 2014). The LHCBM2/7 subunits stabilize the trimeric LHCII and are also part of the PSI–LHCI–LHCII complex, although they may not be themselves phosphorylated (Ferrante et al., 2012; Drop et al., 2014). Supercomplexes of PSI involving the cytochrome b_6f complex can be isolated from cells in St 2 or in anaerobic conditions (Iwai et al., 2010; Steinbeck et al., 2018). They are proposed to facilitate CEF and thus favor the production of ATP. However, the presence and significance of these complexes is still a matter of debate (Buchert et al., 2018).

In vascular plants, the protein kinase STN7 has a paralog called STN8 (Vainonen et al., 2005), which is involved in the phosphorylation of numerous thylakoid proteins, including the core subunits of PSII (Reiland et al., 2011). The protein phosphatase PHOTOSYSTEM II CORE PHOSPHATASE (PBCP) is required for the efficient dephosphorylation of these subunits (Samol et al., 2012; Puthiyaveetil et al., 2014; Liu et al., 2019). While there is some overlap in their substrate specificities, the antagonistic pairs of kinases and phosphatases appear to have fairly distinct roles. STN7 and PPH1/TAP38 are mainly involved in LHCII phosphorylation and state transitions, while STN8 and PBCP influence the architecture of thylakoid membranes and the repair cycle of photoinhibited PSII. In monocots such as rice (*Oryza sativa*), a further role for STN8 and PBCP in the high light-induced phosphorylation of the monomeric LHCII subunit Lhcb4 (CP29) has been proposed (Betterle et al., 2015, 2017; Liu et al., 2019).

While the state-transition kinase STT7 was first identified in *C. reinhardtii* (Depège et al. 2003), the functional homologs of the plant PPH1/TAP38 and PBCP phosphatases have not been characterized yet in the alga. Here we present evidence that in *C. reinhardtii*, homologs of PPH1/TAP38 and PBCP play a role in the regulation of state transitions with partially redundant functions.

RESULTS

CrPPH1 Plays a Role in State Transitions

The closest homolog of the Arabidopsis gene encoding the thylakoid phosphatase PPH1/TAP38 (*At4G27800*) was identified in *C. reinhardtii* as *Cre04.g218150* in reciprocal BLASTP searches (see "Materials and Methods"). The *C. reinhardtii* protein, which we call CrPPH1, shares 36% sequence identity and 55% similarity with its Arabidopsis homolog. To investigate the function of CrPPH1 in *C. reinhardtii*, we obtained a mutant strain from the Chlamydomonas Library Project (CLiP; LMJ.RY0402.16176, https://www.chlamylibrary.org; Li et al., 2016) with a predicted insertion in intron 7 of the *PPH1* gene (Fig. 1A). The site of insertion was confirmed by PCR amplification and sequencing of the amplified product (Supplemental Fig. S1A). This mutant line showed an alteration of state transitions, as will be detailed below. However, according to the CLiP database, this line also carried a second insertion (hereafter *ins2*) in gene *Cre24.g755597.t1.1*, an insertion that was similarly confirmed by PCR analysis (Supplemental Fig. S1B). To remove the second mutation and to test whether the state transition phenotype cosegregated with the *pph1* mutation, the mutant line (*pph1*;*ins2*) was backcrossed twice to the parental strain CC5155 (Supplemental Fig. S1C). From the first cross, 60 complete tetrads were analyzed for paromomycin resistance and for the presence of *pph1* and *ins2* insertions, both of which conferred paromomycin resistance. In eight of these tetrads where the two insertions segregated (non-parental ditypes with four paromomycin-resistant colonies *pph1*/*pph1*/*ins2*/*ins2*), we found that altered state transitions cosegregated with the insertion in the *pph1* gene (Supplemental Fig. S1C). In a second backcross between a *pph1* single mutant deriving from the first backcross and the parental line CC5155, we analyzed eight complete tetrads and observed cosegregation of the insertion in the *pph1* gene with paromomycin resistance and the state transition phenotype (Supplemental Fig. S1D). This analysis shows that the alteration in state transitions is genetically tightly linked to the *pph1* mutation. To facilitate biochemical experiments, we further crossed a *pph1* mutant progeny to the cell-wall–deficient strain *cw15*, and a double mutant, *pph1*;*cw15*, was selected for further analysis. All subsequent experiments were performed comparing the parental *cw15* strain with the double mutant *pph1*;*cw15*; however, hereafter, for simplicity, these strains will be referred to as wild type and *pph1*, respectively. The chlorophyll content and the maximum quantum efficiency of PSII were similar in *pph1* and in the wild type (Supplemental Table S1). The *pph1* mutant also showed normal growth in a variety of conditions (Supplemental Fig. S2).

A rabbit antiserum was raised against recombinant CrPPH1 expressed in *Escherichia coli* (Supplemental Fig. S3A) to assess the presence of the protein by immunoblotting of total protein extracts of the wild type and of the *pph1* mutant (Fig. 1B). A band was observed in the wild type that was not detected in the *pph1* mutant. This band migrated with an apparent molecular mass of 45 kD, somewhat slower compared to the calculated molecular mass of 40 kD for CrPPH1 after removal of a predicted chloroplast transit peptide (cTP) of 52 to 56 amino acid residues according to different algorithms (Predalgo; Tardif et al., 2012; ChloroP; Emanuelsson et al., 1999). Because of the background signal with this antibody, a low level of residual CrPPH1 expression in the *pph1* mutant could not be excluded (Supplemental Fig. S3).

State transitions can be monitored as a change in the fluorescence emission spectrum at 77 K (Fig. 1C). In *C. reinhardtii*, the transitions can be experimentally induced by switching between anaerobic and aerobic conditions. In the dark, anaerobiosis leads to reduction of the PQ pool and consequent establishment of St 2.

Subsequent strong aeration under the light promotes oxidation of the PQ pool and a transition to St 1. The relative sizes of the peaks at 682 nm and 712 nm qualitatively reflect changes in the light harvesting antennae associated with PSII and PSI, respectively. In the wild type, transition from St 2 (LHCII partly connected to PSI) to St 1 (LHCII mostly allocated to PSII) caused a decrease in the PSI peak relative to the PSII peak. The spectrum was recorded after 20 min in the conditions promoting St 1, a timepoint when the transition is nearing completion in the wild type. At this time, the extent of the transition from St 2 toward St 1 was strongly diminished in the *pph1* mutant compared to the wild type (Fig. 1C).

The time courses of state transitions were analyzed in more detail by measuring room-temperature chlorophyll fluorescence using pulse-amplitude-modulation (PAM) spectroscopy (Fig. 1D). Cells that had been acclimated to minimal medium in low light (60 μmol photons m^{-2} s^{-1}) were transferred to the PAM fluorometer and the sample chamber was sealed, so that consumption of oxygen by respiration led to anaerobiosis. Steady-state fluorescence (F_s) was continuously monitored with the low intensity-measuring beam to monitor the redox state of the PQ pool, and saturating flashes were applied every 4 min to measure the maximum fluorescence of PSII ($F_{m'}$), which is related to the cross section of its functional light-harvesting antenna. Reduction of the PQ pool in the dark (denoted by an increase in F_s) triggered the transition to St 2 in the wild type and the *pph1* mutant (decrease of $F_{m'}$). The chamber was then opened, and the algal sample bubbled with air, restoring an aerobic environment and allowing the reoxidation of the PQ pool and a transition toward St 1 (increase of $F_{m'}$). We observed that the transition from St 2 to St 1 was strongly delayed in *pph1* (Fig. 1D), consistent with a role of CrPPH1 in dephosphorylation of the LHCII antenna. A role in state transitions was confirmed using another protocol (Hodges and Barber, 1983; Wollman and Delepelaire, 1984), whereby the transition from St 2 to St 1 was induced by actinic light in the presence of the PSII inhibitor 3-(3,4-dichlorophenyl)-1,1-dimethylurea (DCMU) under continued anaerobiosis (Supplemental Fig. S4). The fact that at the onset of these experiments, *pph1* is capable of a transition from St 1 toward St 2 implies that although the subsequent transition toward St 1 is delayed, *pph1* can eventually reach at least a partial St 1 under the culture conditions used before the measurements (Fig. 1, C and D; Supplemental Fig. S4).

When comparing the two protocols in the wild type (Fig. 1D; Supplemental Fig. S4A), it is interesting to note that the transition from St 2 to St 1 was rapidly induced by aerobiosis (Fig. 1D), but that its onset was delayed a few minutes when it was induced in the presence of DCMU by actinic light under continued anaerobiosis

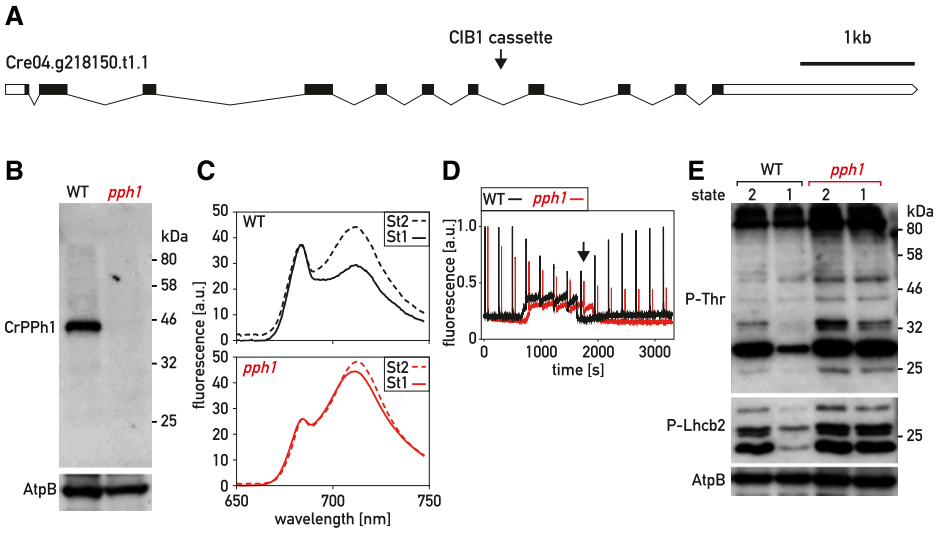

Figure 1. Characterization of the *pph1* mutant. A, Schematic representation of the *PPH1* gene. Exons are represented as black boxes, introns as black lines, and the 5′ untranslated region and 3′ untranslated region as white boxes. The arrowhead indicates the site of insertion of the CIB1 cassette in intron 7. B, Immunoblot analysis. Total protein extracts (50 μg) of the wild type (WT) and of the *pph1* mutant were subjected to SDS-PAGE and immunoblotting with antisera against CrPPH1 or AtpB (loading control). C, Chlorophyll fluorescence emission spectra, 77 K, under conditions that favor St 2 (anaerobiosis in the dark) and after 20 min under conditions that favor St 1 (strong aeration). The data are normalized on the PSII peak at 680 nm. D, State transitions monitored by PAM chlorophyll fluorescence spectroscopy at room temperature. Saturating light flashes were fired every 4 min and fluorescence was measured continuously (no actinic light was applied). Data were normalized on the first $F_{m'}$ peak. The transition from St 1 to St 2 was induced by sealing the sample chamber to allow respiration to deplete oxygen and cause anoxic conditions, and then the transition from St 2 to St 1 was induced by bubbling air in the sample (at the time indicated with a black arrow). E, Phosphoimmunoblot analysis. Total protein extracts (10 μg) of wild-type and *pph1* cells in conditions favoring St 2 or St 1 (as in B) were subjected to SDS-PAGE and immunoblotting with antisera against P-Thr, P-Lhcb2, or AtpB (loading control).

(Supplemental Fig. S4A). This difference might be ascribed to a requirement for both an oxidized PQ pool and sufficient levels of ATP to induce the transition toward St 1 (Bulte et al., 1990). While under restored aerobiosis (Fig. 1D), mitochondrial respiration could rapidly replenish the cellular ATP pool, whereas in the presence of DCMU under anaerobiosis (Supplemental Fig. S4A), CEF would replenish the ATP pool more slowly.

To confirm that this state-transition phenotype is due to the *pph1* mutation, we transformed the mutant strain with a plasmid carrying a wild-type copy of *PPH1* in which we inserted a sequence encoding a triple hemagglutinin (HA) epitope at the 3′ end of the coding sequence (CDS; *PPH1-HA*) and a selection marker (*aph7″*, hygromycin resistance). The transformants were screened by chlorophyll fluorescence spectroscopy, and four lines showing a restoration of state transitions were selected for further analysis. Immunoblotting with a monoclonal HA antibody indicated that the rescued lines (*pph1:PPH1-HA*) expressed the tagged CrPPH1-HA protein, and immunoblotting with the anti-CrPPH1 antibodies showed that the protein was expressed at levels similar to those of the wild type or in moderate excess (Fig. 2A). PAM fluorescence spectroscopy showed that in *pph1:PPH1-HA*, the rate of the transition from St 2 to St 1 was comparable to that of the wild type (Fig. 2B).

To further test the role of CrPPH1 in LHCII dephosphorylation, we examined the phosphorylation status of the major thylakoid proteins by SDS-PAGE and immunoblotting. St 2 was established by anaerobiosis in the dark, and a subsequent transition to St 1 was promoted by strong aeration in the light, as written about above, for the analysis of fluorescence at 77 K. An antibody against phospho-Thr (P-Thr) revealed a complex pattern of phosphoproteins; nevertheless, a distinct decrease in the signal of several bands was observed in the wild type upon transition from St 2 to St 1 (Fig. 1E), as well as in the complemented strains (Fig. 2C). As will be shown below, some of the same bands were clearly underphosphorylated in the mutant *stt7*, which is deficient for the protein kinase involved in state transitions. In the *pph1* mutant, the signal of these phosphoprotein bands decreased much less after switching to the conditions that favor St 1. With an antibody against the phosphorylated form of Arabidopsis Lhcb2 (P-Lhcb2), several bands were observed in *C. reinhardtii*, corresponding to the migration of LHCII (Supplemental Fig. S5), although the sequence divergence between the peptide recognized by the antibody and the potential target sequences in the *C. reinhardtii* antenna subunits does not allow a simple assignment to specific LHCBM isoforms. In the wild type, the intensity of these bands was higher in St 2 than St 1. In the *stt7* mutant (see below), these bands are detected only at low levels that are similar under St-2 or St-1 conditions. These two observations indicate that at least some of the bands revealed in *C. reinhardtii* by the Arabidopsis anti-P-Lhcb2 antibody are implicated in state transitions. These bands were clearly overphosphorylated in *pph1* compared to the wild type in the conditions that favor a transition to St 1. Thus, defects in the dephosphorylation of LHCII antenna components parallel the alteration in state transitions observed spectroscopically in the *pph1* mutant.

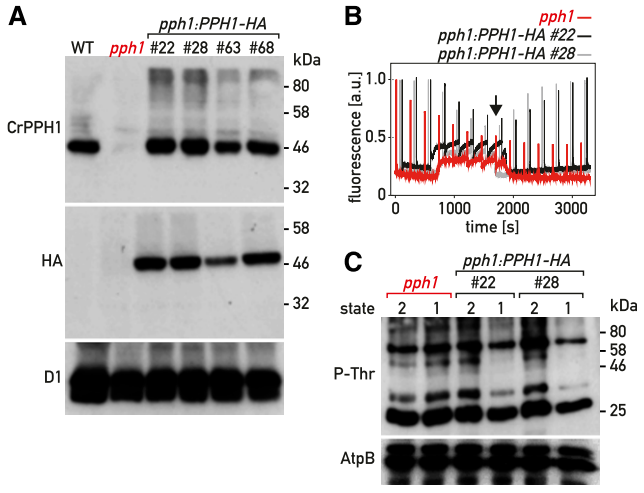

Figure 2. Complementation of the *pph1* mutant. A, Immunoblot analysis. Total protein extracts (50 μg) of the wild type (WT), the *pph1* mutant, and four complemented lines (*pph1:PPH1-HA*) were subjected to SDS-PAGE and immunoblotting with antisera against CrPPH1, the HA epitope, and D1 (loading control). B, State transitions in the *pph1* mutant and two complemented lines were monitored by PAM chlorophyll fluorescence spectroscopy as in Figure 1D. C, Phospho-immunoblot analysis. Total protein extracts (10 μg) of the *pph1* mutant and of complemented lines were subjected to SDS-PAGE and immunoblotting with antisera against P-Thr or AtpB (loading control).

CrPBCP Is Also Involved in State Transitions

A striking feature of the *pph1* mutant was that it showed strong retardation of the transition from St 2 to St 1, but that nevertheless, under normal culture conditions, it was capable of approaching St 1 and undergoing a subsequent transition to St 2 (Fig. 1D; Supplemental Fig. S4). It thus appeared that at least one other protein phosphatase might be involved in state transitions and dephosphorylation of LHCII components, allowing the establishment of St 1 in *pph1*, albeit more slowly. This was corroborated by the identification of another phosphatase mutant affected in state transitions.

A library of mutants with random insertions of an *aphVIII* cassette (paromomycin resistance) was generated and screened using a fluorescence imaging setup (Tolleter et al., 2011). To search for mutants in photoprotective or alternative electron transfer pathways, this library was recently screened again using a different imaging system (Johnson et al., 2009). One of the mutants (identified as *pbcp*, see below) showed impaired transitions from St 2 to St 1 (Fig. 3). Using reverse-PCR techniques, the insertion was mapped to

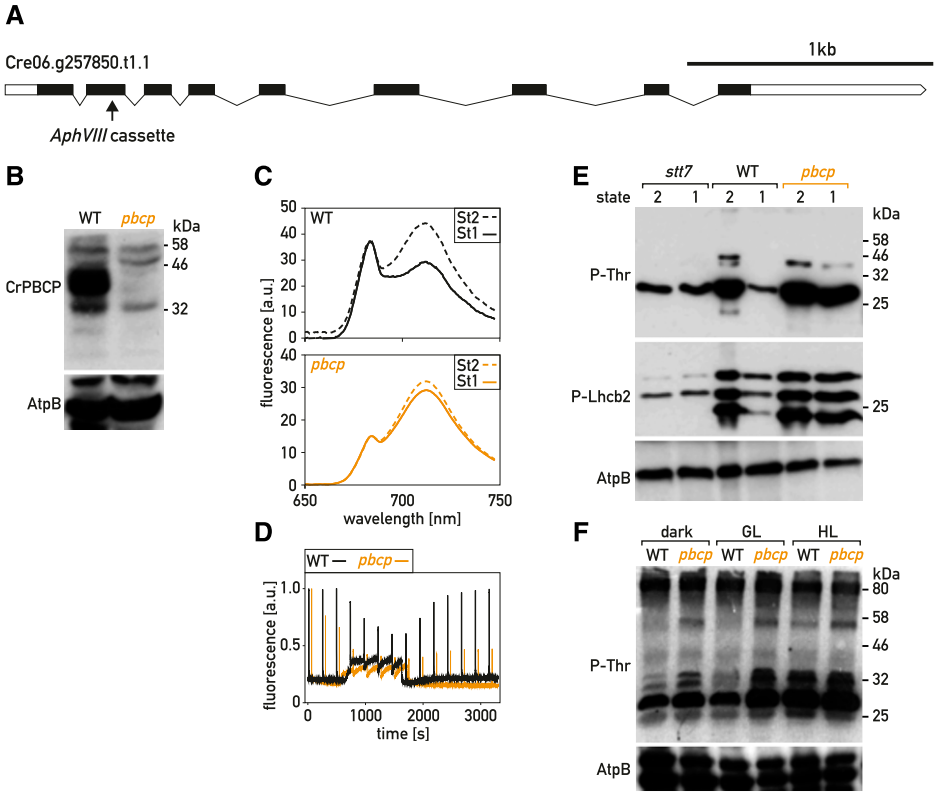

Figure 3. Characterization of the *pbcp* mutant. A, Schematic representation of the *PBCP* gene. Exons are represented as black boxes, introns as black lines, and 3′/5′ untranslated regions as white boxes. The arrow indicates the site of insertion of the *aphVIII* cassette in exon 2. B, Immunoblot analysis. Total protein extracts of the wild type (WT) and of the *pbcp* mutant (50 μg) were subjected to SDS-PAGE and immunoblotting with antisera against PBCP or AtpB (loading control). C, Chlorophyll fluorescence emission spectra, 77 K, under condition that favor St 2 and after 20 min under conditions that favor St 1, as in Figure 1C. D, State transitions of the wild type and the *pbcp* mutant were monitored by PAM chlorophyll fluorescence spectroscopy as in Figure 1D. E, Phospho-immunoblot analysis of state transitions. Total protein extracts of wild type and *pbcp* cells in St 2 and St 1 (10 μg, treated as in Fig. 2C) were subjected to SDS-PAGE and immunoblotting with antisera against P-Thr, P-Lhcb2, or AtpB (loading control). F, Phospho-immunoblot analysis of light acclimation. The cells were grown in low light and then transferred to the dark, growth light (GL, 80 μmol m^{-2} s^{-1}), or high light (HL, 300 μmol m^{-2} s^{-1}) for 2 h and analyzed as in E.

the gene *Cre06.g257850* (Supplemental Fig. S6A), which encodes the *C. reinhardtii* protein most similar to PBCP from Arabidopsis, and will be called CrPBCP hereafter (Fig. 3A). To test whether the alteration of state transitions was genetically linked to the *pbcp* mutation, we backcrossed the mutant to wild-type 137C. In 40 complete tetrads, paromomycin resistance segregated with the insertion in the *PBCP* gene. In the four tetrads that we analyzed further, an overphosphorylation of thylakoid proteins cosegregated with the insertion in *PBCP* (Supplemental Fig. S6B). Moreover, *pbcp* and the phosphorylation phenotype also cosegregated with mating-type minus (mt−), as expected because *PBCP* lies in close proximity to the mating-type locus on chromosome 6. One of the *pbcp* mutant progeny was further crossed to *cw15* to obtain a cell-wall–deficient strain (*pbcp;cw15*), which was used in all subsequent experiments and will be referred to as *pbcp* hereafter. Using a rabbit antiserum raised against recombinant CrPBCP expressed in *E. coli* (Supplemental Fig. S3B) and immunoblotting of total proteins separated by SDS PAGE, the protein was detected in the wild type but not in the *pbcp* mutant (Fig. 3B). The chlorophyll content and the maximum quantum yield of PSII were not significantly different in *pbcp* and in the wild type (Supplemental Table S1). Furthermore, the *pbcp* mutant showed normal growth under a variety of conditions (Supplemental Fig. S2).

We analyzed state transitions in the *pbcp* mutant by determining its fluorescence emission spectra at 77 K in St 2 and after a subsequent transition to conditions promoting St 1 for 20 min. Compared to the wild type, the transition to St 1 was significantly impaired in *pbcp* (Fig. 3C). Using PAM chlorophyll fluorescence spectroscopy, we observed that anaerobiosis in the dark promoted a transition to St 2 in the *pbcp* mutant as in the wild type. However, upon aeration and reoxidation of the PQ pool, the transition from St 2 to St 1 was strongly delayed in *pbcp* (Fig. 3D). Similar observations were made using the protocol where this transition was induced by light in the presence of DCMU (Supplemental Fig. S4). Thus, CrPBCP seems to play a major role in state transitions, unlike its homolog in Arabidopsis.

To confirm that the state-transition phenotype was due to the *pbcp* mutation, we transformed the *pbcp* mutant with a plasmid carrying a wild-type copy of *PBCP* tagged with a sequence encoding a triple HA epitope (*PBCP-HA*) and a selectable marker (*aph7″*). Four rescued lines (*pbcp;PBCP-HA*) that expressed the tagged CrPBCP-HA protein were retained for further analysis. Immunoblotting with the anti-PBCP antibodies (Fig. 4A) showed that the different *pbcp;PBCP-HA* lines expressed the protein at levels similar or somewhat reduced compared to the wild type. State transitions were restored in the *pbcp;PBCP-HA* lines, as monitored by PAM fluorescence spectroscopy (Fig. 4B).

To investigate the alteration of thylakoid protein phosphorylation in the *pbcp* mutant, we used SDS-PAGE and immunoblotting (Fig. 3E). With an anti-P-Thr antibody, we observed that bands that migrate as components of LHCII (Supplemental Fig. S5) were overphosphorylated in *pbcp*, but not in the complemented *pbcp;PBCP-HA* lines (Fig. 4C). Unfortunately, these commercial anti-P-Thr antibodies (now discontinued) did not clearly identify the phosphorylated forms of PSII subunits D2 (PsbD) or CP43 (PsbC; Supplemental Fig. S5). High phosphorylation of LHCII constituents was confirmed with the Arabidopsis anti-P-Lhcb2 antibodies, which showed overphosphorylation in *pbcp* of the bands that are underphosphorylated in the *stt7* mutant. Thus, CrPBCP has a different range of targets in *C. reinhardti* than its homolog in Arabidopsis, where the major targets of PBCP are the subunits of the PSII core. It was striking that excess phosphorylation of thylakoid proteins in *pbcp* appeared not only after a transition from St 2 to St 1, but also under normal growth conditions (80 μmol photons m^{-2} s^{-1}), as well as after growth under high light (300 μmol photons m^{-2} s^{-1}) or in the dark (Fig. 3F).

The *pph1;pbcp* Double Mutant Is Locked in State 2

Both CrPPH1 and CrPBCP are implicated in the dephosphorylation of some components of LHCII and are essential for an efficient transition from St 2 to St 1. Nevertheless, both individual mutants, *pph1* and *pbcp*, are capable of eventually approaching St 1 under the culture conditions before the measurements (Figs. 1D and 3D; Supplemental Fig. S4). To further test whether the two phosphatases play partly redundant roles in the regulation of state transitions, we generated double *pph1;pbcp* mutants by crossing *pph1* and *pbcp* and genotyping the progeny by PCR (Supplemental Fig. S7). The *pph1;pbcp* mutants also carry the *cw15* mutation like both their parents. The double mutants were, as expected, deficient for both CrPPH1 and CrPBCP (Fig. 5A). The maximum quantum yield of PSII and the chlorophyll content of *pph1;pbcp* were not significantly different from the wild type (Supplemental Table S1), and the double mutant showed normal growth under a set of different conditions that were tested (Supplemental Fig. S2).

When state transitions were monitored in *pph1;pbcp* double mutants, it was remarkable that, after preacclimation under low light where the wild-type cells are in St 1, the double mutant had a comparatively low value of $F_{m'}$ at the onset of the measurements, indicative of St 2 (Fig. 5B). There was also no significant further drop in $F_{m'}$ when the *pph1;pbcp* sample became anaerobic with the concomitant rise in F_s. The double mutant also showed no rise in $F_{m'}$ when the sample was aerated again, indicating that the transition to St 1 was severely hampered. Similar results were obtained when this state transition was promoted by light in the presence of DCMU (Supplemental Fig. S4). The low level of $F_{m'}$ indicative of St 2 was matched by a high phosphorylation of LHCII components (Fig. 5C). In contrast to the wild type that showed low phosphorylation in St 1, high phosphorylation after a transition to St 2, and again, low phosphorylation after a further transition to St 1, *pph1;pbcp* showed in all three conditions a phosphorylation pattern similar to that of the wild type in St 2 (Fig. 5C). These observations indicated that the *pph1;pbcp* double mutant is essentially locked in St 2. In further support of this conclusion, we determined the fluorescence emission spectrum at 77 K of cells in all three conditions (St 1 > St 2 > St 1), and observed that

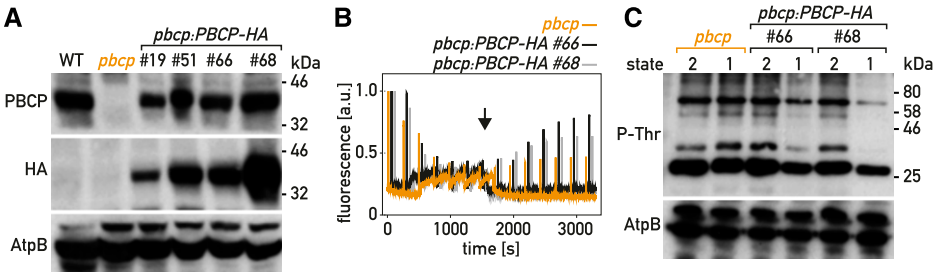

Figure 4. Complementation of the *pbcp* mutant. A, Immunoblot analysis. Total protein extracts (50 μg) of the wild type (WT), the *pbcp* mutant, and four complemented lines (*pbcp:PBCP-HA*) were subjected to SDS-PAGE and immunoblotting with antisera against CrPBCP, the HA epitope, or AtpB (loading control). B, State transitions in the *pbcp* mutant and two complemented lines were monitored by PAM chlorophyll fluorescence spectroscopy at room temperature as in Figure 1D. C, Phospho-immunoblot analysis. Total protein extracts (10 μg) of the *pbcp* mutant and of complemented lines were subjected to SDS-PAGE and immunoblotting with antisera against P-Lhcb2, P-Thr, and AtpB (loading control).

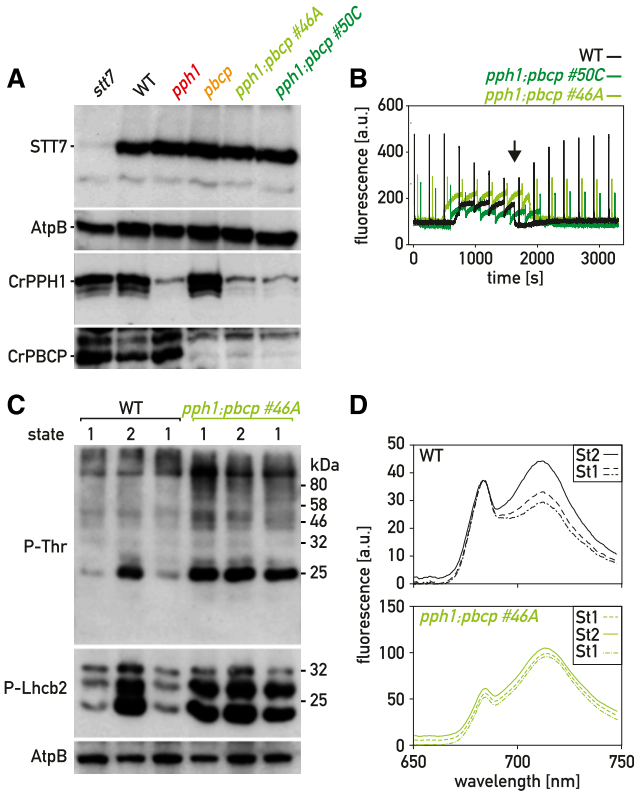

Figure 5. Characterization of the *pph1;pbcp* double mutant. A, Immunoblot analysis. Total protein extracts (50 μg) of *stt7*, wild type (WT), *pph1*, *pbcp*, and *pph1;pbcp* (clones 46A and 50C) were subjected to SDS-PAGE and immunoblotting with antisera against STT7, AtpB (loading control), CrPPH1, and CrPBCP. B, State transitions of the wild type and two *pph1;pbcp* mutants were monitored by PAM chlorophyll fluorescence spectroscopy at room temperature, as in Figure 1D. The data were not normalized to the first $F_{m'}$ peak. C, Phospho-immunoblot analysis. Total protein extracts of wild-type and *pph1;pbcp* cells in conditions favoring St 1, then St 2, and finally again St 1 (10 μg; cells treated as in Fig. 1C) were subjected to SDS-PAGE and immunoblotting with antisera against P-Thr, P-Lhcb2, or AtpB (loading control). D, Chlorophyll fluorescence emission spectra, 77 K, under conditions sequentially favoring St 1, St 2, and St1, obtained as in Figure 1C.

in the *pph1;pbcp* double mutant the fluorescence emission peak of PSI relative to PSII was always larger than in the wild type (Fig. 5D; Supplemental Fig. S4B). Our data indicate that two partially redundant protein phosphatases, CrPPH1 and CrPBCP, are involved in the transition from St 2 to St 1.

Accumulation of Thylakoid Proteins in the Mutants

In Arabidopsis, the expression of STN7 is reduced under prolonged exposure to far-red light (Willig et al., 2011), and the amount of PPH1 is downregulated at a posttranscriptional level in the *psal* mutant, which is deficient in the docking of LHCII to PSI and thus incapable of completing state transitions (Rantala et al., 2016). These observations prompted us to determine whether, in *Chlamydomonas*, the amounts of STT7, CrPPH1, or CrPBCP are altered in the single kinase or phosphatase mutants and also in the *pph1;pbcp* double mutant, using SDS PAGE and immunoblotting of protein extracts from cells grown under normal conditions (Fig. 5A). However, no major differences were observed in the accumulation of the three regulatory proteins.

We also investigated the possibility that the phosphatase mutations might be compensated in the long term by changes in the stoichiometry of the photosystems or other major photosynthetic complexes. Proteins extracts of the wild type, the single mutants *pph1* and *pbcp*, and the double mutant *pph1;pbcp* grown under normal conditions were compared by SDS PAGE and immunoblotting (Supplemental Fig. S8). Antisera against representative subunits of the major complexes were used for this analysis: AtpB (ATP synthase), D1 (PSII), PsaA (PSI), Cytf (cytochrome b_6f complex), and COXIIb (mitochondrial cytochrome oxidase). However, no significant differences were apparent in the relative amounts of the photosynthetic complexes in the mutant lines.

CrPPH1 and CrPBCP Have Overlapping But Distinct Dephosphorylation Targets

In *C. reinhardtii*, LHCII is composed of monomeric LHCB4 (CP29) and LHCB5 (CP26) as well as trimers of isoforms LHCBM1 through LHCBM9. Based on their primary sequences, the trimer subunits belong to four types (Supplemental Fig. S9): type I in which three subgroups can be distinguished (LHCBM3; LHCBM4/LHCBM6/LHCBM8; LHCBM9), type II (LHCBM5), type III (LHCBM2/LHCBM7, which are identical in mature sequence), and type IV (LHCBM1). While the P-Thr antiserum and the Arabidopsis P-Lhcb2 antiserum showed clear differences in the patterns of LHCII phosphorylation in St 1 in both phosphatase mutants (Fig. 6A), the ill-defined specificity of these antisera did not allow the discrimination of the different components of the antenna, or reveal any target specificity of the respective phosphatases. To address these questions, we used Phos-tag PAGE followed by immunoblotting with specific antibodies. We obtained previously described antisera against LHCB4, LHCB5 and LHCBM5 (type II; Takahashi et al., 2006), and also generated antisera against peptides that are characteristic for the other types of LHCBM subunits. Because these isoforms share a high degree of sequence similarity, the antigenic peptides were selected in the N-terminal region of the proteins, which is the most divergent between LHCII types (Supplemental Fig. S9). The specificity of the affinity-purified antibodies was tested against the recombinant LHCII subunits expressed in *E. coli* (Supplemental Fig. S10). The antisera against LHCBM1 (type IV), LHCBM3 (type I), and LHCB4 and LHCB5 (minor antenna) proved to be very specific. The antiserum against LHCBM2/7 (type III) showed minor cross reactions toward type-I isoforms.

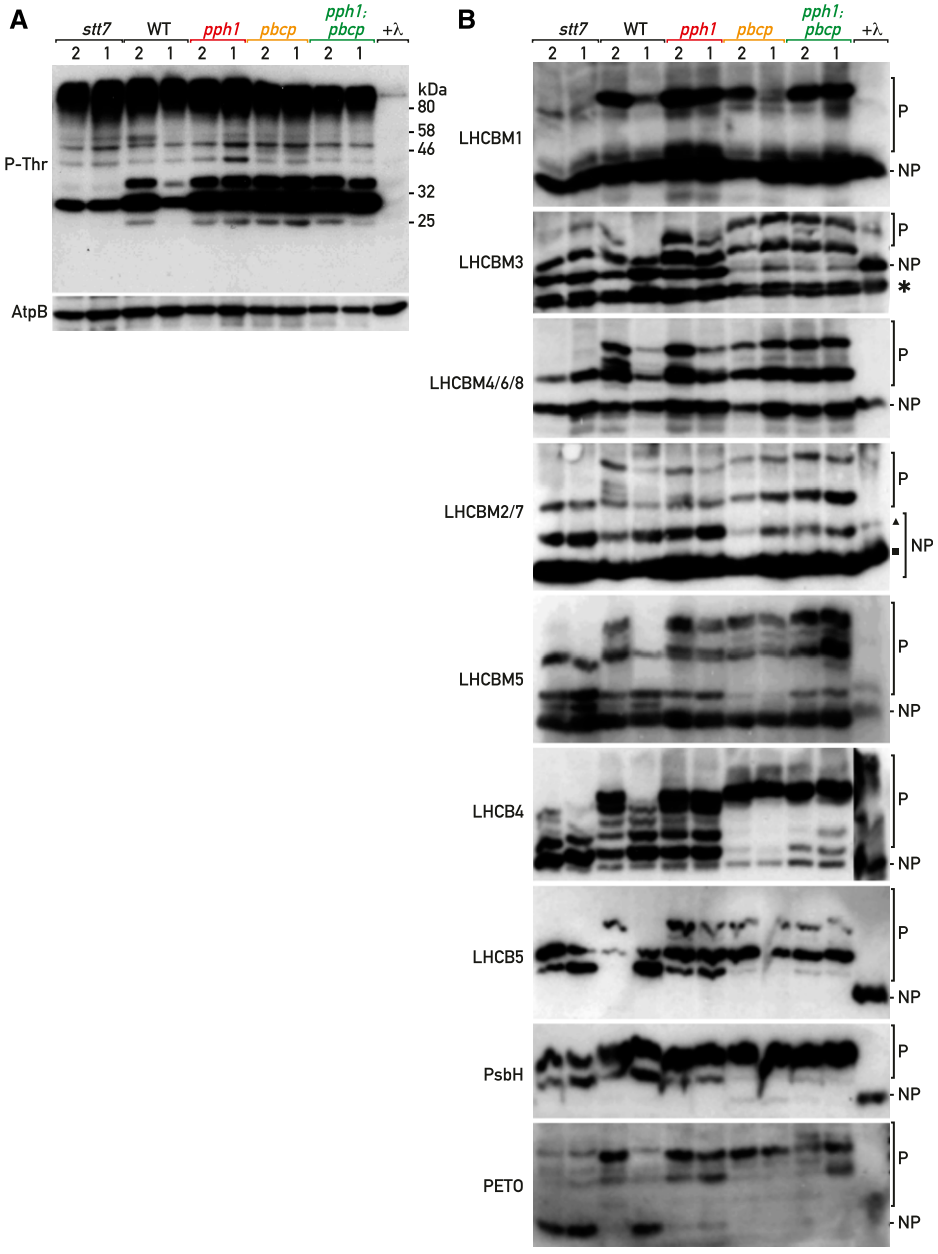

Figure 6. Analysis of CrPPH1 and CrPBCP targets. A, Phospho-immunoblot analysis. Total protein extracts of *stt7*, wild type (WT), *pph1*, *pbcp*, and *pph1*;*pbcp* (10 μg) in conditions favoring St 2 and then St 1 were subjected to SDS-PAGE and immunoblotting with antisera against P-Thr or AtpB (loading control). B, Phos-tag PAGE and immunoblot analysis. Total protein extracts (10 μg) of *stt7*, wild type, *pph1*, *pbcp*, or *pph1*;*pbcp* in St 2 and then St 1 were subjected to Phos-tag PAGE and immunoblotting with antisera against LHCBM1, LHCBM3, LHCBM4/6/8, LHCBM2/7, LHCBM5, LHCB4, LHCB5, PsbH, or PETO. A sample of the wild type in St 2 was treated with lambda phosphatase (+λ) and used as a reference for the migration of the non-phosphorylated (NP) form. The migration of the phosphorylated (P) forms is retarded by the Phos-tag immobilized in the polyacrylamide gel.

Finally, the antiserum against LHCBM4/6/8 (type I, which shares the same sequence in the N-terminal region) also reacted toward LHCBM3 (also type I), but unexpectedly very strongly decorated LHCBM9 (type I). It should be noted, however, that LHCBM9 is only expressed under conditions of nutrient stress (Grewe et al., 2014).

To analyze the phosphorylation of the different proteins by immunoblotting, we used Phos-tag, which is a metal chelator that can be cross linked into a polyacrylamide gel during polymerization (Kinoshita et al., 2009). This chelator binds Zn^{2+} ions that interact with phosphate groups and thus retards the migration of phosphorylated forms of proteins during SDS-PAGE. After immunoblotting (Fig. 6B), the degree of phosphorylation of the target protein is reflected in the ratio of the bands representing one or more slower-migrating phospho-form(s) to the band corresponding to the faster-migrating nonphosphorylated protein. To determine the migration of the nonphosphorylated form, we treated a sample of the wild type in St 2 with a nonspecific protein phosphatase (λ-phosphatase) before electrophoresis (lane marked λ in Fig. 6B).The antipeptide antibodies are targeted to the N terminus of the LHCBM subunits, which also contains the major sites of phosphorylation. To avoid any bias due to differential recognition by these antibodies of the phosphorylated and nonphosphorylated forms of their targets, we treated the proteins after blotting onto the membrane with λ-phosphatase (Longoni et al., 2015).

Because the phosphatases play a role in the transition from St 2 to St 1, we analyzed protein extracts of the wild type and the different mutants in St 2 (induced by anaerobiosis in the dark) and after a subsequent transition to St 1 (triggered by aerating the sample).

The antibodies against LHCBM1 (type IV) labeled two bands in the wild type in St 2 (Fig. 6B). The lower one comigrated with the single band in the λ-phosphatase–treated sample, representing the nonphosphorylated protein. The upper band, corresponding to a phosphorylated form, gave a strong signal relative to the lower one, indicative of a high degree of LHCBM1 phosphorylation in St 2. The ratio of the phosphorylated band to the nonphosphorylated one was much lower in the kinase mutant *stt7*, or after the transition to St 1. In the *pph1* mutant, strong phosphorylation of LHCBM1 was still apparent in the conditions promoting St 1, with a high ratio of the upper to the lower band, in contrast to the wild type or the *pbcp* mutant. The double mutant *pph1*;*pbcp* showed the same high degree of phosphorylation after the transition to St-1 conditions as the *pph1* mutant. We infer that CrPPH1 is a major actor of LHCBM1 dephosphorylation during the transition to St 1.

The antibodies against LHCBM3 (type I) decorated two bands after Phos-tag gel electrophoresis of the λ-phosphatase–treated sample (Fig. 6B), as well as after conventional gel electrophoresis of an untreated sample (Supplemental Fig. S8B), even though these antibodies were specific for LHCBM3 among the recombinant proteins expressed in *E. coli* (Supplemental Fig. S10). The lower band (marked with an asterisk), which was partially resolved as a doublet, is unlikely to represent processed forms of LHCBM3 lacking amino acid residues at the N terminus (Stauber et al., 2003), because the LHCBM3 antibodies were raised against this region and would not recognize a truncated protein. Thus, the lower band may reflect nonspecific binding to another protein. There were two additional slower-migrating bands in the wild type in St 2, largely absent from the λ-phosphatase–treated sample, suggesting that LHCBM3 may undergo phosphorylation at more than one site, or that the nonspecific protein is phosphorylated as well. One of these bands was also clearly present in *stt7*, suggesting the involvement of another protein kinase in LHCBM3 phosphorylation. The relative intensity of the top-most of the phosphorylated bands to the nonphosphorylated ones clearly decreased after transition to St 1 in the wild type. Some dephosphorylation was still apparent in the *pph1* mutant, but the overall phosphorylation level appeared to be higher. In contrast, the *pbcp* mutant showed a much higher ratio of phosphorylated bands in both St 2 and St 1, as did the *pph1*;*pbcp* double mutant. Thus, CrPBCP appears to play the major role for dephosphorylation of LHCBM3.

With the antibodies against LHCBM4/6/8 (type I), a single major band was observed in the λ-phosphatase–treated sample (Fig. 6B), as well as after conventional gel electrophoresis (Supplemental Fig. S8B). However, these antibodies also recognized other recombinant type-I isoforms, LHCBM3 and LHCBM9 (Supplemental Fig. S10). The latter should not be expressed under our conditions, because it is induced by nutrient stress (Grewe et al., 2014). After Phos-tag electrophoresis of the wild-type sample in St 2, the pattern of phosphorylation was complex, with most bands corresponding to those revealed with anti-LHCBM3 (but excluding the band marked with an asterisk). One of the phosphorylated forms was present in the *stt7* mutant. The degree of phosphorylation of the others decreased in St 1 in both the wild type and *pph1*, but not in *pbcp* or *pph1*;*pbcp* where the most phosphorylated form was prevalent. We tentatively infer that CrPBCP is involved in dephosphorylation of LHCBM4/6/8 and, because it also affects LHCBM3, more generally in the dephosphorylation of type-I isoforms.

The antibodies against LHCBM2/7 (type III) decorated a strong band in the λ-phosphatase–treated sample, with a second minor band above it. Likewise, after conventional gel electrophoresis, these antibodies labeled a major and a minor band (Supplemental Fig. S8B). Among the recombinant proteins expressed in *E. coli*, the LHCBM2/7 antibodies strongly recognized LHCBM2/7 but also weakly cross reacted with the type-I isoforms LHCBM3, LHCBM4/6/8, and LHCBM9 (Supplemental Fig. S10). The patterns of the phosphorylated bands, together with the upper nonphosphorylated band (marked with a triangle) but excluding the strong nonphosphorylated band below (marked with a square), were similar to the pattern obtained with anti-LHCBM4/6/8, and may mostly represent the cross reaction to these isoforms (Fig. 6B). Compared to LHCBM4/6/8, the strong additional nonphosphorylated band (marked with a square) can tentatively be ascribed to LHCBM2/7, which is thus apparently not subject to phosphorylation under these conditions, or only to a small degree.

With antiserum against LHCBM5 (type II), two bands were detected in the λ-phosphatase–treated sample, and at least five more in the various genotypes in St 2 (Fig. 6B). Two bands were also observed after conventional SDS-PAGE (Supplemental Fig. S8B), which could represent processed forms of LHCBM5 or cross reactions to other isoforms, so it is unclear which of the five upper bands correspond to phosphorylated LHCBM5. The four uppermost bands were missing in *stt7*, suggesting that their phosphorylation relates to state-transitions. In the wild type in St 1 and in *stt7*, an additional band was present between the two nonphosphorylated ones, likely representing a low-phosphorylation form. Higher ratios of the upper bands to the lower ones were observed in St 1 in *pph1* and *pbcp*, and an even higher ratio in *pph1*;*pbcp*. These observations suggest that both CrPPH1 and CrPBCP act in a partly redundant manner on the phosphorylation of LHCBM5, and potentially other cross-reacting proteins decorated by the antibody.

Antiserum against LHCB4, which recognized a single band after conventional SDS-PAGE (Supplemental

Fig. S8B), decorated multiple bands in the wild type in St 2 (Fig. 6B), in accordance with the multiple phosphorylation sites that have been observed in LHCB4 (Lemeille et al., 2010). The upper bands were missing in *stt7*, and the ratio of the upper ones to the lower ones decreased in the wild type in St 1 compared to St 2. In *pph1*, the pattern in St 1 resembled that of St 2, while in *pbcp*, as well as in *pph1;pbcp*, a very high degree of phosphorylation was observed in both states. These data suggest that CrPPH1 and CrPBCP contribute to LHCB4 dephosphorylation in St 1, and that CrPBCP may play such a role also in St 2, independently of state transitions.

The antiserum against LHCB5, which labels a single band after conventional SDS-PAGE (Supplemental Fig. S8B), decorated at least three bands in the different samples, none of which comigrated with the non-phosphorylated form in the λ-phosphatase–treated sample (Fig. 6B). Two of the constitutively phosphorylated forms were present in *stt7*, while the third and slowest-migrating form was present in the wild type in St 2 but not in St 1. The latter was still present in *pph1* in St 1, while it became prevalent compared to the lowest one in *pbcp*, and in *pph1;pbcp*. These observations suggest that CrPPH1 and CrPBCP participate in LHCB5 dephosphorylation in St 1, and that CrPBCP may also contribute in St 2.

With antiserum against the PsbH subunit of PSII, two phosphorylated forms were observed in the wild type and in *stt7*, in both St-2 and St-1 conditions (Fig. 6B). Phosphorylation appeared stronger in *pbcp* as well as *pph1;pbcp*, suggesting that CrPBCP is probably involved in the dephosphorylation of PsbH, like its homolog in Arabidopsis (Samol et al., 2012).

Finally, with antiserum against PETO, which is a phospho-protein implicated in the regulation of CEF (Hamel et al., 2000; Takahashi et al., 2016), a major phosphorylated form as well as one or two minor ones were observed in the wild type in St 2 that were strongly diminished in St 1 or in the *stt7* mutant. In *pph1* the phosphorylation was retained in St 1, in *pbcp* the upper band became most prevalent, and in *pph1;pbcp*, an even slower-migrating band was apparent. These data indicate that both CrPPH1 and CrPBCP are involved in the dephosphorylation of PETO in a somewhat additive manner.

DISCUSSION

We have identified two protein phosphatases that are required for efficient transitions from St 2 to St 1 in *C. reinhardtii*. CrPPH1 is the closest homolog of Arabidopsis PPH1/TAP38, which is involved in state transitions in plants (Pribil et al., 2010; Shapiguzov et al., 2010). Unexpectedly, we found that in *C. reinhardtii*, CrPBCP is also involved in state transitions. This is in contrast to PBCP from Arabidopsis, which is required for the dephosphorylation of several PSII core subunits but not of the LHCII antenna (Samol et al., 2012). In Arabidopsis, lack of PBCP does not affect state transitions and it is only when this phosphatase is strongly overexpressed that it has a minor effect on the rate of state transitions. In rice, OsPBCP contributes to dephosphorylation of LHCB4 (CP29) and is proposed to have a role in regulating the dissipation of excess energy (Betterle et al., 2017). The different substrate specificities of the two phosphatases from higher plants can be explained by the different geometry of their substrate binding sites (Wei et al., 2015; Liu et al., 2019).

The transition from St 2 to St 1 is strongly delayed in the *pph1* and *pbcp* mutants of *C. reinhardtii*. However after incubation in conditions favoring St 1, both single mutants are nevertheless capable of approaching St 1 (Figs. 1D and 3D; Supplemental Fig. S4) and then undergo a transition toward St 2. In contrast, the double mutant *pph1;pbcp* remains in St 2 even in the conditions that favor St 1 in the wild type (Fig. 5; Supplemental Fig. S4). Thus, the phenotypes of the two mutants show some additivity, but the two phosphatases have partly redundant functions in state transitions.

State transitions are regulated by the phosphorylation or dephosphorylation of LHCII antenna proteins. In Arabidopsis, the Lhcb1 and Lhcb2 components of the LHCII trimers can be phosphorylated, but not Lhcb3, with phospho-Lhcb2 playing a major role in the formation of the PSI–LHCI–LHCII complexes in St 2 (Crepin and Caffarri, 2015; Longoni et al., 2015). To investigate the requirement of CrPPH1 and CrPBCP in antenna dephosphorylation during a transition from St 2 to St 1 in *C. reinhardtii*, we used Phos-tag PAGE and immunoblotting (Fig. 6B). Although some of the anti-peptide antisera that we developed displayed some cross reactions among closely related LHCBM isoforms, it was still possible to assign many phosphorylated forms to the different types of LHCBM. The Phos-tag PAGE technique has the advantage of allowing an assessment of cumulative phosphorylation. Compared to the simple patterns that are obtained with Lhcb1 and Lhcb2 in Arabidopsis (Longoni et al., 2015), with each one having only a single major phosphorylated form, the patterns proved much more complex in *C. reinhardtii*, raising the possibility that some LHCBM isoforms may undergo multiple phosphorylation. The analysis revealed interesting differences and overlaps between the targets of CrPPH1 and CrPBCP. CrPPH1 was essential for dephosphorylation of the type-IV isoform LHCBM1, while mainly CrPBCP was required for dephosphorylation of the type-I isoforms LHCBM3 and LHCBM4/6/8. Both CrPPH1 and CrPBCP were necessary for dephosphorylation of the type-II isoform LHCBM5 as well as the minor antennae LHCB4 and LHCB5, with CrPBCP playing a dominant role for LHCB4. An overphosphorylation phenotype was already apparent in St 2 in the *pbcp* mutant for LHCBM3, LHCB4, and LHCB5 and, although to a lower extent, LHCBM3 and LHCBM5 appeared overphosphorylated in *pph1* under St-2 conditions. After growth under constant condition of low light or high light, overphosphorylation was also observed in the

pbcp mutant by immunoblotting with anti-P-Thr antibodies. It thus appears that CrPBCP may be active in dephosphorylation status of thylakoid proteins not only in conditions that promote St 1, but also under more balanced steady-state conditions.

In Arabidopsis, PPH1 is specific for LHCII, although its strong overexpression has an effect on the dephosphorylation of the PSII core subunits D1 and D2 (Pribil et al., 2010; Shapiguzov et al., 2010). Conversely, PBCP is mostly required for dephosphorylation of PSII subunits (D1, D2, and CP43), but it can also act on LHCII (Samol et al., 2012; Longoni et al., 2019). In *C. reinhardtii*, the major phosphorylated thylakoid proteins include, in addition to LHCII, some subunits of PSII (D2 [PsbD], CP43 [PsbC], and PsbH (Delepelaire, 1984; de Vitry et al., 1991), as well as PETO (Hamel et al., 2000). Using Phos-tag gel electrophoresis, we found that both CrPPH1 and CrPBCP influence not only the dephosphorylation of components of LHCII, but also components of the PsbH subunit of PSII. Phosphorylation of LHCII still occurred in a mutant lacking PSII (Wollman and Delepelaire, 1984), but phosphorylation of PSII did not occur in a mutant lacking LHCII proteins (de Vitry and Wollman, 1988). While the two phosphatases target partially overlapping sets of components of both PSII and LHCII, it seems likely that differences in regulation and target specificities also lie with the protein kinases STT7 and STL1. STT7 appears specific for LHCII (Turkina et al., 2006; Lemeille et al., 2010), while putatively STL1 might phosphorylate PSII, like its paralog STN8 in Arabidopsis (reviewed by Rochaix et al., 2012). We also obtained evidence that both phosphatases are involved in the dephosphorylation of PETO, which is implicated in the control of CEF (Takahashi et al., 2016). In summary, CrPBCP and CrPPH1 seem to have distinct but overlapping sets of targets, with CrPBCP having a somewhat wider spectrum. Whether these targets represent direct substrates of the phosphatases or indirect targets through regulatory cascades cannot be determined from our genetic analysis.

In *C. reinhardtii*, LHCBM5, CP29, and CP26 were enriched in PSI–LHCI–LHCII complexes in St 2 (Takahashi et al., 2006, 2014), although all types of LHCBM could also be found (Drop et al., 2014). Genetic studies have shown that type-III isoform LHCBM2/7, type-I isoforms LHCBM4/6/8, and CP29 and CP26 are implicated in state transitions (Tokutsu et al., 2009; Ferrante et al., 2012; Girolomoni et al., 2017; Cazzaniga et al., 2020). We observed that, with the possible exception of LHCBM2/7, all types of LHCBMs as well as LHCB4 and LHCB5 are differentially phosphorylated in St 2 compared to St 1. In particular, we found that LHCBM1 was phosphorylated in St 2, that its phosphorylation depends on STT7, and that it was dephosphorylated in St 1, mainly reliant on CrPPH1. However mutants that lack LHCBM1 were previously found to perform state transitions (Ferrante et al., 2012). Taken together, these observations beg the question of the physiological role of LHCBM1 phosphorylation. A possible explanation might be that, for state transitions, LHCBM1 phosphorylation acts redundantly with the phosphorylation of other antenna proteins, so that they can fulfill this role in the mutants lacking LHCBM1. Analysis of knock-down mutants indicated that LHCBM2/7 is important for state transitions (Ferrante et al., 2012). The comparison of the data we obtained with the antibodies against LHCBM2/7 and LHCBM4/6/8 suggests that the type-III isoform LHCBM2/7 may not be phosphorylated in St 2, which is consistent with the previous report that phosphorylation of LHCBM2/7 is not detected in the PSI–LHCI–LHCII complex (Drop et al., 2014). A possible reason might be that LHCBM2/7 could be required structurally for the association of LHCII trimers to PSI–LHCI, but that this isoform would not be involved in regulation through phosphorylation. This would be analogous to the case in Arabidopsis, where Lhcb1 is not phosphorylated when it is a component of the mobile LHCII trimer that binds to PSI–LHCI, so that it is only the phosphorylation of Lhcb2 that is required for binding of LHCII to the PSI docking site (Crepin and Caffarri, 2015; Longoni et al., 2015; Pan et al., 2018).

Compared to Arabidopsis, *C. reinhardtii* lacks LHCB6 (CP24) but has a more complex complement of the LHCBM subunits composing the LHCII trimers (reviewed by Crepin and Caffarri, 2018). Another difference is that in *C. reinhardtii*, some PSI–LHCI–LHCII complexes contain not only LHCII trimers but also the "minor" antennae LHCB4 and LHCB5 (Drop et al., 2014; Takahashi et al., 2014). Furthermore, the amplitude of state transitions is larger in *C. reinhardtii* than in plants (Delosme et al., 1996), and in the alga, strong state transitions are induced by changes in metabolic demands for ATP or reducing power, for example under anoxic conditions (Bulte and Wollman, 1990; Cardol et al., 2009). It remains a matter of speculation whether these differences are related to the more intricate roles of the phosphatases CrPPH1 and CrPBCP in the regulation of light harvesting that have evolved in *C. reinhardtii*. On the other hand, in *C. reinhardtii*, phosphorylation of LHCB4 is controlled by CrPBCP, reminiscent of monocots such as rice where phosphorylation of LHCB4 is controlled by OsSTN8 and OsPBCP (Betterle et al., 2017). Further "evo-physio" investigations from a combined evolutionary and physiological perspective on the role of protein phosphorylation in the regulation of photosynthetic acclimation in diverse organisms promise to be a fertile approach.

MATERIALS AND METHODS

Strains, Growth Conditions, and Media

The *Chlamydomonas reinhardtii cw15.16* (*mt+*) mutant was obtained by crossing *cw15* (*mt−*) to wild-type 137C. The *C. reinhardtii* CLiP strain LMJ.RY0402.16176, its parental strain CC4533 (*mt−*), and the corresponding strain of opposite mating type CC5155 (*mt+*) were obtained from the Chlamydomonas Resource Center (https://www.chlamycollection.org/; Li et al., 2016). This CLiP strain (*pph1;cao*) was backcrossed twice to CC4533, and then to

cw15 to obtain the cell-wall–deficient mutant strain *pph1;cw15* used in this work and referred to as *pph1*. The *pbcp* strain was isolated by screening random insertional mutants for aberrant chlorophyll-fluorescence induction kinetics. These mutants were generated by inserting an *aphVIII* cassette in wild-type 137C (*mt*−; Tolleter et al., 2011). The *pbcp* mutant was backcrossed with wild-type 137C (*mt*+), and further to *cw15.16* (*mt*+) to obtain the cell-wall–deficient mutant strain *pbcp;cw15* used in this work and referred to as *pbcp*. The genotype of the progeny was verified by PCR (see below) and the phenotype by monitoring state transitions using PAM chlorophyll fluorescence spectroscopy (see below).

Cells were grown in Tris acetate phosphate (TAP; Harris, 1989) under normal growth light (60–80 μmol m^{-2} s^{-1}) from white fluorescent tubes. The state transitions were obtained with cells in exponential growth phase (two to three 10^6 cells/mL) collected by centrifugation, resuspended in High Salt Minimal medium at a concentration of two to three 10^7 cells per mL, and preacclimated in dim light (~10 μmol m^{-2} s^{-1}) for 2 h with shaking.

Mapping of the Insertion in *pbcp*

DNA was isolated using the cetyltrimethylammonium bromide method and quantified using a NanoDrop spectrophotometer (Thermo Fisher Scientific). The Resda-PCR protocol was used to identify the left border, and the technique was adapted from González-Ballester et al. (2005). The first PCR was performed with Taq polymerase and 10% (w/v) DMSO, using DegAluI (degenerate primer) and RB1 (primer on the *aphVIII* cassette). The program included five cycles with annealing at 58°C, then 20 repetitions at 25°C, and then at 55°C for one cycle, at 58°C for two cycles, and at 40°C for one cycle. A second nested PCR was performed on the product of the first PCR diluted to 1/1,000 using KOD Xtreme Hot Start DNA Polymerase (Merck Millipore) and primers Q_o and RB2 (González-Ballester et al., 2005). The product of the second PCR was then loaded onto an agarose gel (2% [w/v]), and fragments with a $M_r > 800$ bp were isolated. PCR products were extracted from the gel and purified with NucleoSpin Gel and a PCR Clean-up Kit (Macherey Nagel), and eluted in water before sequencing. The Genome Walker technique (Clontech) was used to identify the right border of the flanking sequence of the cassette insertion site. Genomic DNA was successively digested using the enzyme *Pvu*II followed by the ligation of a specific adapter. The primary PCR uses a primer specific to the insert (AphVIII) and an adapter-specific primer. This was followed by a nested PCR whereby products >800 bp were extracted from agarose gel and cloned. Cloning of the PCR products was performed in the vector pGEM-T (Promega) containing the lactose operon and the gene coding for ampicillin resistance, and then transformed into chemo-competent *Escherichia coli* (DH5) by thermal shock. The bacteria were selected on luria broth Ampicillin medium in the presence of β-D-1-ThioGalactopyranoside and 5-bromo-4-chloro-3-indolyl-beta-D-galactopyranoside to allow for white/blue selection.

DNA Constructs

The protein with the highest sequence similarity to Arabidopsis (*Arabidopsis thaliana*) PPH1/TAP38 (At4G27800) was identified in *C. reinhardtii* as Cre04.g218150 in reciprocal BLAST searches performed in Phytozome 12 (E-value: 6. E-57; https://phytozome.jgi.doe.gov/pz/portal.html#!search?show=BLAST) and The Arabidopsis Information Resource (TAIR 10; E-value: 9. E-56; http://www.arabidopsis.org/Blast/index.jsp).

Vector pPL18 was obtained from pSL18 by replacing the *aphVIII* resistance cassette with the hygromycin resistance cassette (Sizova et al., 2001). For this, the *aphVIII* cassette was removed by *Kpn*I/*Xho*I digestion. The hygromycin cassette was amplified from plasmid MAC1_gen3 (Douchi et al., 2016) with primers pPL 56 and pPL 57 (see Supplemental Table S2) and cloned by Gibson assembly (Gibson et al. (2009)).

The vector was further modified to allow the fusion of a triple HA epitope tag at the C terminus of the CDSs of interest. A synthetic fragment encoding the triple epitope (obtained from Biomatik) was cloned into pPL18 by *Bsm*I/*Not*I digestion, yielding vector pFC18.

The *CrPPH1* CDS was amplified from a *C. reinhardtii* complementary DNA library with primers pFC_216 and pFC_217 and cloned by Gibson assembly into pFC18 linearized with *Eco*RV/*Bgl*II, resulting in pFC18_CrPPH1_HA. The *CrPBCP* CDS was amplified from a complementary DNA library with primers pFC_218 and pFC_219 and cloned as above, into pFC18 resulting in pFC18_CrPBCP_HA. The *CrPPH1* CDS without the predicted cTP was amplified with primer pFC_265 and primer pFC_266 from pFC18_CrPPH1_HA, then cloned into vector pet28a digested with *Nde*I and *Sal*I to obtain pet28a_CrPPH1_ΔcTP. The *CrPBCP* CDS without the predicted cTP was amplified with primer pFC_267 and primer pFC_268 from pFC18_CrPBCP_HA, and cloned into pet28a as above to obtain pET28a_CrPBCP_ΔcTP. All vectors used were verified by sequencing.

Transformation

Nuclear transformation by electroporation was modified from Shimogawara et al. (1998). Cells in exponential phase were collected by centrifugation and resuspended at 10^8 cell per mL in TAP + 60 mM Suc. A volume of 300 μL of cells was incubated with 1 μg of plasmid DNA (linearized with *Xba*I) at 16°C for 20 min, and then the mix was transferred to a 4-mm–gap electroporation cuvette and pulsed at 500 V (C = 50 μF) using a GenePulser II electroporator (Bio-Rad). The cuvette was then incubated at 16°C for 20 min. The cell suspension was diluted into 20 mL of TAP, then incubated in dim light with gentle agitation for 16 h and collected by centrifugation, before plating and selection, on TAP + 25 μg mL^{-1} hygromycin (Sigma-Aldrich).

Production of Polyclonal Antiserum of CrPPH1, CrPBCP, and LHCBMs

For production of CrPPH1 and CrPBCP, recombinant proteins were expressed from plasmids pet28a-CrPPH1_ΔcTP and pET28a-CrPBCP_ΔcTP in *E. coli* BL21(DE3) induced with 1 mM of β-D-1-ThioGalactopyranoside for 4 h at 37°C. Recombinant proteins purified as in Ramundo et al. (2013) were used to immunize rabbits, and antisera were purified by affinity chromatography with the corresponding protein (Eurogentec).

For production of antipeptide antisera targeting different LHCBMs isoforms (Natali and Croce, 2015), synthetic peptides (Supplemental Fig. S9) were used for rabbit immunization and affinity chromatography (Eurogentec). For assessing the specificity and cross reaction of the antibodies, pET28a plasmids carrying the CDSs of LHCBM1, LHCBM2, LHCBM3, LHCBM4, LHCBM5, LHCBM6, LHCBM9, CP26, and CP29 (Girolomoni et al., 2017) were used to express all the antenna proteins in *E. coli* BL21(DE3).

Fluorescence Measurements

Maximum quantum efficiency of PSII (F_v/F_m) of cells that were adapted for ~1 to 5 min in the dark was measured with a plant efficiency analyzer (Handy PEA; Hansatech Instruments) with the parameters recommended by the manufacturer. State transitions were monitored with a PAM fluorometer (Hansatech Instruments). A 2-mL sample of cells grown and preacclimated in High Salt Minimal medium as described above was transferred to the dark in the vessel of a PAM fluorometer (Hansatech Instruments). The sample was kept in the dark with stirring, and saturating pulses (pulse width of 0.7 s; intensity 85%) were applied every 4 min. The St-1 to St-2 transition was induced by sealing the chamber, so that respiration led to anoxic conditions, and then the transition from St 2 to St 1 was induced by bubbling air in the sample. The alternate protocol for inducing state transitions in the presence of DCMU is described in Supplemental Figure S4. Chlorophyll fluorescence emission spectra at 77 K were measured with a spectrofluorometer (Ocean Optics) with excitation from an LED light source at 435 nm.

Immunoblotting

For total protein extraction, cells in exponential phase were collected by centrifugation, resuspended in lysis buffer (50 mM of Tris-HCl at pH 6.8, 2% [w/v] SDS, and 10 mM of EDTA) and 1× Protease inhibitor cocktail (Sigma-Aldrich) and incubated at 37°C for 30 min with shaking in a thermomixer. Cell debris was removed by centrifugation at 16,000*g* for 10 min at 4°C, and the supernatant was used as total protein extract. For protein phosphorylation analysis, any centrifugation step of living cells was avoided by instantly dousing the cultures in 4 vol of cold acetone. After 30-min incubation on ice and centrifugation at 12,000*g* for 12 min in an SLA-4 rotor (Sorvall), the pellet was treated as before. Samples (10 or 50 μg of total protein) were denaturated for 30 min at 37°C before SDS-PAGE (Laemmli, 1970) in 15% or 12% (w/v) acrylamide gels. After wet transfer, the nitrocellulose membranes (Bio-Rad) were blocked in TBS plus TWEEN (20 mM of Tris at pH 7.5, 150 mM of NaCl, and 0.1% [v/v] TWEEN 20) supplemented with 5% (w/v) nonfat milk (or 3% [w/v] BSA in the case of anti-P-Thr immunoblotting), for 2 h at room temperature or 16 h at 4°C.

The antisera (and their sources) were as follows: monoclonal anti-HA (Promega); anti-phospho-LHCB2 (AS13-2705; Agrisera); anti-PsaA (a gift of

Kevin Redding); anti-Cytf and anti-D1 (gifts of Jean-David Rochaix); anti-Phospho Thr (Invitrogen); anti-LHCB4, anti-LHCB5, and anti-LHCBM5 (gifts of Yuichiro Takahashi); anti-rabbit IgG horseradish peroxidase conjugate (Promega); and anti-mouse IgG horseradish peroxidase conjugate (Promega). For primary antibody decoration, antibodies were diluted in the same buffers as for blocking, and incubation was for 2 h at room temperature or 16 h at 4°C. Membranes were washed four times for 8 min with TBS-T and then incubated 1 h at room temperature with horseradish-peroxidase–conjugated secondary antibody diluted in TBS-T with 5% (w/v) nonfat milk (or 3% [w/v] BSA in the case of anti-P-Thr immunoblotting). Membranes were washed four times for 8 min with TBS-T and then revealed by enhanced chemiluminescence.

Phos-Tag Gel Electrophoresis

Double-layer Phos-tag gels (12% [w/v] acrylamide/bisacrylamide 37.5:1 and 65 μM of Phos-Tag; Wako Pure) were prepared as in Longoni et al. (2015), except that the presence of EDTA in the lysis buffer was compensated by adding equimolar $Zn(NO_3)_2$ to the samples, and denaturated for 30 min at 37°C before loading. Protein dephosphorylation on the membranes was performed as in Longoni et al. (2015). For in vitro dephosphorylation, a cell pellet was resuspended in 5 mM of HEPES at pH 7.5, 10 mM of EDTA, and 1% (v/v) TritonX 100, and an aliquot containing 10 μg of protein was treated with lambda protein phosphatase reaction mix following the instructions of the manufacturer (New England Biolabs) for 1 h at 30°C.

Accession Numbers

Sequence data from this article can be found in the Joint Genome Institute Phytozome data libraries (https://phytozome.jgi.doe.gov/pz/portal.html) under the accession numbers PPH1, Cre04.g218150; PBCP, Cre06.g257850; LHCBM1, Cre01.g066917; LHCBM2, Cre12.g548400; LHCBM3, Cre04.g232104; LHCBM4, Cre06.g283950; LHCBM5, Cre03.g156900; LHCBM6, Cre06.g285250; LHCBM7, Cre12.g548950; LHCBM8, Cre06.g284250; and LHCBM9, Cre06.g284200.

Supplemental Data

The following materials are available.

Supplemental Figure S1. Genotyping of two insertions in the *pph1* mutant, and segregation analysis.

Supplemental Figure S2. Growth properties of the single and double mutants.

Supplemental Figure S3. Validation of CrPPH1 and CrPBCP antisera.

Supplemental Figure S4. Time course of state transitions in the presence of DCMU and corresponding fluorescence emission spectra at 77 K.

Supplemental Figure S5. Migration of selected thylakoid proteins after SDS-PAGE.

Supplemental Figure S6. Identification of the *pbcp* mutant, and segregation analysis.

Supplemental Figure S7. Genotyping of *pph1;pbcp* double mutants.

Supplemental Figure S8. Accumulation of photosynthetic proteins in the single and double mutants.

Supplemental Figure S9. Design of peptide antigens for antisera against LHCBM isoforms.

Supplemental Figure S10. Specificity and cross reactions of the antisera against LHCII components.

Supplemental Table S1. Chlorophyll content and maximum quantum yield of PSII in the phosphatase mutants.

Supplemental Table S2. List of oligonucleotides used in this work.

ACKNOWLEDGMENTS

We thank Jean-David Rochaix, Jean Alric, Bernard Genty, and Gilles Peltier for scientific advice; Pascaline Auroy for technical assistance; Matteo Ballottari for the plasmids expressing LHCBMs; Francis-André Wollman for antiserum against PETO; Yuichiro Takahashi for antisera against CP29, CP26, and LHCBM5; and Nicolas Roggli for help with preparing the figures.

Received March 30, 2020; accepted April 9, 2020; published April 23, 2020.

LITERATURE CITED

Bassi R, Wollman FA (1991) The chlorophyll-*a*/*b* proteins of Photosystem II in *Chlamydomonas reinhardtii*: Isolation, characterization and immunological cross-reactivity to higher-plant polypeptides. Planta **183:** 423–433

Bellafiore S, Barneche F, Peltier G, Rochaix JD (2005) State transitions and light adaptation require chloroplast thylakoid protein kinase STN7. Nature **433:** 892–895

Benson SL, Maheswaran P, Ware MA, Hunter CN, Horton P, Jansson S, Ruban AV, Johnson MP (2015) An intact Light Harvesting Complex I antenna system is required for complete state transitions in Arabidopsis. Nat Plants **1:** 15176

Betterle N, Ballottari M, Baginsky S, Bassi R (2015) High light-dependent phosphorylation of Photosystem II inner antenna CP29 in monocots is STN7 independent and enhances nonphotochemical quenching. Plant Physiol **167:** 457–471

Betterle N, Poudyal RS, Rosa A, Wu G, Bassi R, Lee CH (2017) The STN8 kinase-PBCP phosphatase system is responsible for high-light-induced reversible phosphorylation of the PSII inner antenna subunit CP29 in rice. Plant J **89:** 681–691

Buchert F, Hamon M, Gäbelein P, Scholz M, Hippler M, Wollman FA (2018) The labile interactions of cyclic electron flow effector proteins. J Biol Chem **293:** 17559–17573

Bulte L, Gans P, Rebeille F, Wollman FA (1990) ATP control on state transitions in vivo in *Chlamydomonas reinhardtii*. Biochim Biophys Acta **1020:** 72–80

Bulte L, Wollman FA (1990) Stabilization of state I and state II by p-benzoquinone treatment of intact cells of *Chlamydomonas reinhardtii*. Biochim Biophys Acta **1016:** 253–258

Cardol P, Alric J, Girard-Bascou J, Franck F, Wollman FA, Finazzi G (2009) Impaired respiration discloses the physiological significance of state transitions in Chlamydomonas. Proc Natl Acad Sci USA **106:** 15979–15984

Cazzaniga S, Kim M, Bellamoli F, Jeong J, Lee S, Perozeni F, Pompa A, Jin E, Ballottari M (2020) Photosystem II antenna complexes CP26 and CP29 are essential for nonphotochemical quenching in *Chlamydomonas reinhardtii*. Plant Cell Environ **43:** 496–509

Crepin A, Caffarri S (2015) The specific localizations of phosphorylated LHCB1 and LHCB2 isoforms reveal the role of LHCB2 in the formation of the PSI–LHCII supercomplex in Arabidopsis during state transitions. Biochim Biophys Acta **1847:** 1539–1548

Crepin A, Caffarri S (2018) Functions and evolution of LHCB isoforms composing LHCII, the major light harvesting complex of Photosystem II of green eukaryotic organisms. Curr Protein Pept Sci **19:** 699–713

Delepelaire P (1984) Partial characterization of the biosynthesis and integration of the Photosystem II reaction centers in the thylakoid membrane of *Chlamydomonas reinhardtii*. EMBO J **3:** 701–706

Delosme R, Olive J, Wollman FA (1996) Changes in light energy distribution upon state transitions: An in vivo photoacoustic study of the wild type and photosynthesis mutants from *Chlamydomonas reinhardtii*. Biochim Biophys Acta Bioenerg **1273:** 150–158

Depège N, Bellafiore S, Rochaix JD (2003) Role of chloroplast protein kinase Stt7 in LHCII phosphorylation and state transition in Chlamydomonas. Science **299:** 1572–1575

de Vitry C, Diner BA, Popo JL (1991) Photosystem II particles from *Chlamydomonas reinhardtii*. Purification, molecular weight, small subunit composition, and protein phosphorylation. J Biol Chem **266:** 16614–16621

de Vitry C, Wollman FA (1988) Changes in phosphorylation of thylakoid membrane-proteins in light-harvesting complex mutants from *Chlamydomonas reinhardtii*. Biochim Biophys Acta **933:** 444–449

Douchi D, Qu Y, Longoni P, Legendre-Lefebvre L, Johnson X, Schmitz-Linneweber C, Goldschmidt-Clermont M (2016) A nucleus-encoded chloroplast phosphoprotein governs expression of the Photosystem I subunit PsaC in *Chlamydomonas reinhardtii*. Plant Cell **28:** 1182–1199

Drop B, Webber-Birungi M, Fusetti F, Kouřil R, Redding KE, Boekema EJ, Croce R (2011) Photosystem I of *Chlamydomonas reinhardtii* contains nine light-harvesting complexes (LHCA) located on one side of the core. J Biol Chem **286:** 44878–44887

Drop B, Yadav K N S, Boekema EJ, Croce R (2014) Consequences of state transitions on the structural and functional organization of Photosystem I in the green alga *Chlamydomonas reinhardtii*. Plant J **78:** 181–191

Dumas L, Zito F, Blangy S, Auroy P, Johnson X, Peltier G, Alric J (2017) A stromal region of cytochrome b_6f subunit IV is involved in the activation of the Stt7 kinase in Chlamydomonas. Proc Natl Acad Sci USA **114:** 12063–12068

Eberhard S, Finazzi G, Wollman FA (2008) The dynamics of photosynthesis. Annu Rev Genet **42:** 463–515

Elrad D, Grossman AR (2004) A genome's-eye view of the light-harvesting polypeptides of *Chlamydomonas reinhardtii*. Curr Genet **45:** 61–75

Emanuelsson O, Nielsen H, von Heijne G (1999) ChloroP, a neural network-based method for predicting chloroplast transit peptides and their cleavage sites. Protein Sci **8:** 978–984

Ferrante P, Ballottari M, Bonente G, Giuliano G, Bassi R (2012) LHCBM1 and LHCBM2/7 polypeptides, components of major LHCII complex, have distinct functional roles in photosynthetic antenna system of *Chlamydomonas reinhardtii*. J Biol Chem **287:** 16276–16288

Finazzi G, Rappaport F, Furia A, Fleischmann M, Rochaix JD, Zito F, Forti G (2002) Involvement of state transitions in the switch between linear and cyclic electron flow in *Chlamydomonas reinhardtii*. EMBO Rep **3:** 280–285

Fleischmann MM, Ravanel S, Delosme R, Olive J, Zito F, Wollman FA, Rochaix JD (1999) Isolation and characterization of photoautotrophic mutants of *Chlamydomonas reinhardtii* deficient in state transition. J Biol Chem **274:** 30987–30994

Galka P, Santabarbara S, Khuong TT, Degand H, Morsomme P, Jennings RC, Boekema EJ, Caffarri S (2012) Functional analyses of the plant Photosystem I-light-harvesting complex II supercomplex reveals that light-harvesting complex II loosely bound to Photosystem II is a very efficient antenna for Photosystem I in state II. Plant Cell **24:** 2963–2978

Gibson DG, Young L, Chuang RY, Venter JC, Hutchison CA III, Smith HO (2009) Enzymatic assembly of DNA molecules up to several hundred kilobases. Nat Methods **6:** 343–345

Girolomoni L, Ferrante P, Berteotti S, Giuliano G, Bassi R, Ballottari M (2017) The function of LHCBM4/6/8 antenna proteins in *Chlamydomonas reinhardtii*. J Exp Bot **68:** 627–641

Goldschmidt-Clermont M, Bassi R (2015) Sharing light between two photosystems: Mechanism of state transitions. Curr Opin Plant Biol **25:** 71–78

González-Ballester D, de Montaigu A, Galván A, Fernández E (2005) Restriction enzyme site-directed amplification PCR: A tool to identify regions flanking a marker DNA. Anal Biochem **340:** 330–335

Grewe S, Ballottari M, Alcocer M, D'Andrea C, Blifernez-Klassen O, Hankamer B, Mussgnug JH, Bassi R, Kruse O (2014) Light-harvesting complex protein LHCBM9 is critical for Photosystem II activity and hydrogen production in *Chlamydomonas reinhardtii*. Plant Cell **26:** 1598–1611

Hamel P, Olive J, Pierre Y, Wollman FA, de Vitry C (2000) A new subunit of cytochrome b_6f complex undergoes reversible phosphorylation upon state transition. J Biol Chem **275:** 17072–17079

Harris EH (1989) The Chlamydomonas Sourcebook A Comprehensive Guide to Biology and Laboratory Use. Academic Press, San Diego, CA

Hodges M, Barber J (1983) State 1–state 2 transitions in a unicellular green algae: Analysis of in vivo chlorophyll fluorescence induction curves in the presence of 3-(3,4-dichlorophenyl)-1, 1-dimethylurea (DCMU). Plant Physiol **72:** 1119–1122

Houille-Vernes L, Rappaport F, Wollman FA, Alric J, Johnson X (2011) Plastid terminal oxidase 2 (PTOX2) is the major oxidase involved in chlororespiration in Chlamydomonas. Proc Natl Acad Sci USA **108:** 20820–20825

Iwai M, Roth MS, Niyogi KK (2018) Subdiffraction-resolution live-cell imaging for visualizing thylakoid membranes. Plant J **96:** 233–243

Iwai M, Takizawa K, Tokutsu R, Okamuro A, Takahashi Y, Minagawa J (2010) Isolation of the elusive supercomplex that drives cyclic electron flow in photosynthesis. Nature **464:** 1210–1213

Johnson X, Vandystadt G, Bujaldon S, Wollman FA, Dubois R, Roussel P, Alric J, Béal D (2009) A new setup for in vivo fluorescence imaging of photosynthetic activity. Photosynth Res **102:** 85–93

Kinoshita E, Kinoshita-Kikuta E, Koike T (2009) Separation and detection of large phosphoproteins using Phos-tag SDS-PAGE. Nat Protoc **4:** 1513–1521

Kubota-Kawai H, Burton-Smith RN, Tokutsu R, Song C, Akimoto S, Yokono M, Ueno Y, Kim E, Watanabe A, Murata K, et al (2019) Ten antenna proteins are associated with the core in the supramolecular organization of the Photosystem I supercomplex in *Chlamydomonas reinhardtii*. J Biol Chem **294:** 4304–4314

Laemmli UK (1970) Cleavage of structural proteins during the assembly of the head of bacteriophage T4. Nature **227:** 680–685

Lemeille S, Turkina MV, Vener AV, Rochaix JD (2010) Stt7-dependent phosphorylation during state transitions in the green alga *Chlamydomonas reinhardtii*. Mol Cell Proteomics **9:** 1281–1295

Li X, Zhang R, Patena W, Gang SS, Blum SR, Ivanova N, Yue R, Robertson JM, Lefebvre PA, Fitz-Gibbon ST, et al (2016) An indexed, mapped mutant library enables reverse genetics studies of biological processes in *Chlamydomonas reinhardtii*. Plant Cell **28:** 367–387

Liu X, Chai J, Ou X, Li M, Liu Z (2019) Structural insights into substrate selectivity, catalytic mechanism, and redox regulation of rice Photosystem II core phosphatase. Mol Plant **12:** 86–98

Longoni P, Douchi D, Cariti F, Fucile G, Goldschmidt-Clermont M (2015) Phosphorylation of the light-harvesting complex II isoform LHCB2 is central to state transitions. Plant Physiol **169:** 2874–2883

Longoni P, Samol I, Goldschmidt-Clermont M (2019) The kinase state transition 8 phosphorylates light harvesting complex II and contributes to light acclimation in *Arabidopsis thaliana*. Front Plant Sci **10:** 1156

Mazor Y, Borovikova A, Nelson N (2015) The structure of plant Photosystem I super-complex at 2.8 Å resolution. eLife **4:** e07433

Merchant SS, Prochnik SE, Vallon O, Harris EH, Karpowicz SJ, Witman GB, Terry A, Salamov A, Fritz-Laylin LK, Maréchal-Drouard L, et al (2007) The Chlamydomonas genome reveals the evolution of key animal and plant functions. Science **318:** 245–250

Minagawa J, Takahashi Y (2004) Structure, function and assembly of Photosystem II and its light-harvesting proteins. Photosynth Res **82:** 241–263

Nagy G, Ünnep R, Zsiros O, Tokutsu R, Takizawa K, Porcar L, Moyet L, Petroutsos D, Garab G, Finazzi G, et al (2014) Chloroplast remodeling during state transitions in *Chlamydomonas reinhardtii* as revealed by noninvasive techniques in vivo. Proc Natl Acad Sci USA **111:** 5042–5047

Natali A, Croce R (2015) Characterization of the major light-harvesting complexes (LHCBM) of the green alga *Chlamydomonas reinhardtii*. PLoS One **10:** e0119211

Nawrocki WJ, Santabarbara S, Mosebach L, Wollman FA, Rappaport F (2016) State transitions redistribute rather than dissipate energy between the two photosystems in Chlamydomonas. Nat Plants **2:** 16031

Ozawa SI, Bald T, Onishi T, Xue H, Matsumura T, Kubo R, Takahashi H, Hippler M, Takahashi Y (2018) Configuration of ten light-harvesting chlorophyll a/b complex I subunits in *Chlamydomonas reinhardtii* Photosystem I. Plant Physiol **178:** 583–595

Pan X, Ma J, Su X, Cao P, Chang W, Liu Z, Zhang X, Li M (2018) Structure of the maize Photosystem I supercomplex with light-harvesting complexes I and II. Science **360:** 1109–1113

Pietrzykowska M, Suorsa M, Semchonok DA, Tikkanen M, Boekema EJ, Aro EM, Jansson S (2014) The light-harvesting chlorophyll a/b binding proteins Lhcb1 and Lhcb2 play complementary roles during state transitions in Arabidopsis. Plant Cell **26:** 3646–3660

Pribil M, Pesaresi P, Hertle A, Barbato R, Leister D (2010) Role of plastid protein phosphatase TAP38 in LHCII dephosphorylation and thylakoid electron flow. PLoS Biol **8:** e1000288

Puthiyaveetil S, Woodiwiss T, Knoerdel R, Zia A, Wood M, Hoehner R, Kirchhoff H (2014) Significance of the Photosystem II core phosphatase PBCP for plant viability and protein repair in thylakoid membranes. Plant Cell Physiol **55:** 1245–1254

Ramundo S, Rahire M, Schaad O, Rochaix JD (2013) Repression of essential chloroplast genes reveals new signaling pathways and regulatory feedback loops in Chlamydomonas. Plant Cell **25:** 167–186

Rantala M, Lehtimäki N, Aro EM, Suorsa M (2016) Downregulation of TAP38/PPH1 enables LHCII hyperphosphorylation in Arabidopsis mutant lacking LHCII docking site in PSI. FEBS Lett **590:** 787–794

Reiland S, Finazzi G, Endler A, Willig A, Baerenfaller K, Grossmann J, Gerrits B, Rutishauser D, Gruissem W, Rochaix JD, et al (2011) Comparative phosphoproteome profiling reveals a function of the STN8

kinase in fine-tuning of cyclic electron flow (CEF). Proc Natl Acad Sci USA **108:** 12955–12960

Rochaix JD (2014) Regulation and dynamics of the light-harvesting system. Annu Rev Plant Biol **65:** 287–309

Rochaix JD, Lemeille S, Shapiguzov A, Samol I, Fucile G, Willig A, Goldschmidt-Clermont M (2012) Protein kinases and phosphatases involved in the acclimation of the photosynthetic apparatus to a changing light environment. Philos Trans R Soc Lond B Biol Sci **367:** 3466–3474

Samol I, Shapiguzov A, Ingelsson B, Fucile G, Crèvecoeur M, Vener AV, Rochaix JD, Goldschmidt-Clermont M (2012) Identification of a Photosystem II phosphatase involved in light acclimation in Arabidopsis. Plant Cell **24:** 2596–2609

Shapiguzov A, Ingelsson B, Samol I, Andres C, Kessler F, Rochaix JD, Vener AV, Goldschmidt-Clermont M (2010) The PPH1 phosphatase is specifically involved in LHCII dephosphorylation and state transitions in Arabidopsis. Proc Natl Acad Sci USA **107:** 4782–4787

Shimogawara K, Fujiwara S, Grossman A, Usuda H (1998) High-efficiency transformation of *Chlamydomonas reinhardtii* by electroporation. Genetics **148:** 1821–1828

Sizova I, Fuhrmann M, Hegemann P (2001) A *Streptomyces rimosus* aphVIII gene coding for a new type phosphotransferase provides stable antibiotic resistance to *Chlamydomonas reinhardtii*. Gene **277:** 221–229

Stauber EJ, Fink A, Markert C, Kruse O, Johanningmeier U, Hippler M (2003) Proteomics of *Chlamydomonas reinhardtii* light-harvesting proteins. Eukaryot Cell **2:** 978–994

Steinbeck J, Ross IL, Rothnagel R, Gäbelein P, Schulze S, Giles N, Ali R, Drysdale R, Sierecki E, Gambin Y, et al (2018) Structure of a PSI–LHCI–cyt b_6f supercomplex in *Chlamydomonas reinhardtii* promoting cyclic electron flow under anaerobic conditions. Proc Natl Acad Sci USA **115:** 10517–10522

Takahashi H, Clowez S, Wollman FA, Vallon O, Rappaport F (2013) Cyclic electron flow is redox-controlled but independent of state transition. Nat Commun **4:** 1954

Takahashi H, Iwai M, Takahashi Y, Minagawa J (2006) Identification of the mobile light-harvesting complex II polypeptides for state transitions in *Chlamydomonas reinhardtii*. Proc Natl Acad Sci USA **103:** 477–482

Takahashi H, Okamuro A, Minagawa J, Takahashi Y (2014) Biochemical characterization of Photosystem I-associated light-harvesting complexes I and II isolated from state 2 cells of *Chlamydomonas reinhardtii*. Plant Cell Physiol **55:** 1437–1449

Takahashi H, Schmollinger S, Lee JH, Schroda M, Rappaport F, Wollman FA, Vallon O (2016) PETO interacts with other effectors of cyclic electron flow in Chlamydomonas. Mol Plant **9:** 558–568

Takahashi Y, Yasui TA, Stauber EJ, Hippler M (2004) Comparison of the subunit compositions of the PSI–LHCI supercomplex and the LHCI in the green alga *Chlamydomonas reinhardtii*. Biochemistry **43:** 7816–7823

Tapie P, Choquet Y, Breton J, Delepelaire P, Wollman FA (1984) Orientation of Photosystem-I pigments. Investigation by low-temperature linear dichroism and polarized fluorescence emission. Biochim Biophys Acta Bioenerg **767:** 57–69

Tardif M, Atteia A, Specht M, Cogne G, Rolland N, Brugière S, Hippler M, Ferro M, Bruley C, Peltier G, et al (2012) PredAlgo: A new subcellular localization prediction tool dedicated to green algae. Mol Biol Evol **29:** 3625–3639

Tokutsu R, Iwai M, Minagawa J (2009) CP29, a monomeric light-harvesting complex II protein, is essential for state transitions in *Chlamydomonas reinhardtii*. J Biol Chem **284:** 7777–7782

Tolleter D, Ghysels B, Alric J, Petroutsos D, Tolstygina I, Krawietz D, Happe T, Auroy P, Adriano JM, Beyly A, et al (2011) Control of hydrogen photoproduction by the proton gradient generated by cyclic electron flow in *Chlamydomonas reinhardtii*. Plant Cell **23:** 2619–2630

Turkina MV, Kargul J, Blanco-Rivero A, Villarejo A, Barber J, Vener AV (2006) Environmentally modulated phosphoproteome of photosynthetic membranes in the green alga *Chlamydomonas reinhardtii*. Mol Cell Proteomics **5:** 1412–1425

Ünlü C, Drop B, Croce R, van Amerongen H (2014) State transitions in *Chlamydomonas reinhardtii* strongly modulate the functional size of Photosystem II but not of Photosystem I. Proc Natl Acad Sci USA **111:** 3460–3465

Vainonen JP, Hansson M, Vener AV (2005) STN8 protein kinase in *Arabidopsis thaliana* is specific in phosphorylation of Photosystem II core proteins. J Biol Chem **280:** 33679–33686

Vener AV, van Kan PJ, Rich PR, Ohad I, Andersson B (1997) Plastoquinol at the quinol oxidation site of reduced cytochrome bf mediates signal transduction between light and protein phosphorylation: thylakoid protein kinase deactivation by a single-turnover flash. Proc Natl Acad Sci USA **94:** 1585–1590

Wei X, Guo J, Li M, Liu Z (2015) Structural mechanism underlying the specific recognition between the Arabidopsis state-transition phosphatase TAP38/PPH1 and phosphorylated light-harvesting complex protein LHCB1. Plant Cell **27:** 1113–1127

Willig A, Shapiguzov A, Goldschmidt-Clermont M, Rochaix JD (2011) The phosphorylation status of the chloroplast protein kinase STN7 of Arabidopsis affects its turnover. Plant Physiol **157:** 2102–2107

Wlodarczyk LM, Snellenburg JJ, Ihalainen JA, van Grondelle R, van Stokkum IH, Dekker JP (2015) Functional rearrangement of the light-harvesting antenna upon state transitions in a green alga. Biophys J **108:** 261–271

Wollman FA, Delepelaire P (1984) Correlation between changes in light energy distribution and changes in thylakoid membrane polypeptide phosphorylation in *Chlamydomonas reinhardtii*. J Cell Biol **98:** 1–7

Yadav KN, Semchonok DA, Nosek L, Kouřil R, Fucile G, Boekema EJ, Eichacker LA (2017) Supercomplexes of plant Photosystem I with cytochrome b_6f, light-harvesting complex II and NDH. Biochim Biophys Acta Bioenerg **1858:** 12–20

Yamori W, Shikanai T (2016) Physiological functions of cyclic electron transport around Photosystem I in sustaining photosynthesis and plant growth. Annu Rev Plant Biol **67:** 81–106

Zito F, Finazzi G, Delosme R, Nitschke W, Picot D, Wollman FA (1999) The Q_o site of cytochrome b_6f complexes controls the activation of the LHCII kinase. EMBO J **18:** 2961–2969